NASA TM-77741

NASA TECHNICAL MEMORANDUM

NASA TM-77741

SHEAR-LAYER CORRECTION AFTER AMIET UNDER CONSIDERATION OF ADDITIONAL TEMPERATURE GRADIENT. WORKING DIAGRAMS FOR CORRECTION OF SIGNALS

W. Dobrzynski

Translation of "Scherschichtkorrektur nach Amiet unter Berucksichtigung einer zusatzlichen Temperaturscherschicht. Arbeitsdiagramme fur die Korrektur, Deutsche", Forschungs-Versuchsanstalt fuer Luft- und Raumfahrt, Institut fuer Entwurfsaerodynamik Braunschweig, West Germany, (Background information related ICAO CAEP WG II Meeting, Boston, MA, 21-23 May, 1984), March 1984, pp. 1-60.

NATIONAL AERONAUTICS AND SPACE ADMINISTRATION
WASHINGTON D. C. 20546 JULY 1984

STANDARD TITLE PAGE

1. Report No. NASA TM-77741	2. Government Accession No.	3. Recipient's Catalog No.
4. Title and Subtitle SHEAR-LAYER CORRECTION AFTER AMIET UNDER CONSIDERATION OF ADDITIONAL TEMPERATURE GRADIENT. WORKING DIAGRAMS FOR CORRECTION OF SIGNALS		5. Report Date July, 1984 6. Performing Organization Code
7. Author(s) W. Dobrzynski		8. Performing Organization Report No. 10. Work Unit No.
9. Performing Organization Name and Address SCITRAN Box 5456 Santa Barbara, CA 93108		11. Contract or Grant No. NASw 3542 13. Type of Report and Period Covered Translation
12. Sponsoring Agency Name and Address National Aeronautics and Space Administration Washington, D.C. 20546		14. Sponsoring Agency Code

15. Supplementary Notes Translation of "Scherschichtkorrektur nach Amiet unter Berucksichtigung einer zusatzlichen Temperaturscherschicht. Arbeitsdiagramme fur die Korrektur, Deutsche", Forschungs-Versuchsanstalt fuer Luft- und Raumfahrt, Institut fuer Entwurfsaerodynamik Braunschweig, West Germany, (Background information related ICAO CAEP WG II Meeting, Boston, MA, 21-23 May, 1984), March 1984, pp. 1-60.

16. Abstract Amiet's correction scheme for sound wave transmission through shear-layers is extended to incorporate the additional effects of different temperatures in the flow-field in the surrounding medium at rest. Within a parameter-regime typical for acoustic measurements in wind tunnels amplitude-and angle-correction is calculated and plotted systematically to provide a data base for the test engineer.

17. Key Words (Selected by Author(s))	18. Distribution Statement
	Unclassified and Unlimited

19. Security Classif. (of this report)	20. Security Classif. (of this page)	21. No. of Pages	22. Price
Unclassified	Unclassified	55	

N-154,811
N85-12654#

Pages 2-4 intentionally left blank.

Table of Contents

This page intentionally left blank.

Notation

c	m/s	Speed of sound
h	m	Separation of sound source from the shear layer
M	-	Mach number
P_A	N/m²	Acoustic pressure at the point (A)
P_M	N/m²	Acoustic pressure at the measurement point (M)
P_{c-}	N/m²	Acoustic pressure immediately ahead of the shear layer (on the source side)
P_{c+}	N/m²	Acoustic pressure adjacent to the rear of the shear layer (measurement side)
t	K	Temperature
U	m/s	Flow speed
x,y,z	m	Cartesian coordinates
x_o	m	Axial separation of the sound source from the intersection point of a sound ray with the shear layer
Y	m	Side separation of the measurement point from the sound source
α	deg.	Angle between wave front and shear layer
μ	- $=(t_i/t_a)^{1/2}$	
φ	deg.	Angle between the shear layer and the sound propagation direction in the surrounding medium at rest
φ'	deg.	Through radiation angle from the sound source in the flow
φ_M	deg.	Angle betweeen the connection line of sound source-measurement point and the shear layer
ρ	kg/m³	Density

Subscripts

i	-	In the flow
a	-	In the surrounding medium at rest

This page intentionally left blank.

1. Introduction

/9*

When studying aeroacoustic phenomena using wind tunnel tests (free jet configuration), often one measures the acoustic field outside of the wind tunnel flow which is produced by the noise source inside the flow. The acoustic signal has to pass through the flow shear layer of the wind tunnel free jet on its way to the measurement microphone. Consequently, there is a change in the pressure amplitude and in the original radiation direction.

In order to obtain accurate measurement data, additional corrections are required. From the large number of research papers published on this topic, the method of Amiet [1] published in the last few years and its correction method has proven itself. It has been systematically tested already by experimental investigations [2]. The correction equations given by Amiet, however, are restricted to the case of uniform temperature in the wind tunnel flow and the surrounding medium. The theory, which is the basis of the correction method, however, does not require this restriction, which was already noticed by Amiet.

During investigations, in a free jet wind tunnel, especially in large facilities, it is easy for a temperature difference between the flow and the surroundings to occur, or the temperature of the air flow is used as a parameter in aeroacoustic measurements. Therefore, in the present paper, we will extend the correction equations of Amiet for sound propagation through a wind tunnel shear layer to the influence of different temperatures in the flow and the surroundings. In particular, we will then give a systematic result presentation to the test engineer, which will enable him to perform a fast correction of the measured data.

---

* Numbers in margin indicate foreign pagination

2. Expansion of the Correction Method of Amiet to Different Temperatures Inside and Outside of the Flow /10

The correction method of Amiet is based on a paper by Ribner [3], in which the amplitude changes and angular changes when a plane acoustic wave passes through an infinitesimally thin and plane flow shear layer are given. Amiet, in his paper [1], relates this solution to laws of geometric acoustics. In particular, he allows the shear layer to be located in the near field of the acoustic source. In the following we will give a theoretical derivation of the correction equations for the changes of the acoustic propagation direction and pressure amplitude, with the additional influence of an infinitesimally thin temperature shear layer as well. The theoretical expansion, however, will be restricted to steps in which the temperature influence becomes effective. The complete derivation of the theoretical relationships can be found in the literature [1 and 3].

2.1 Theoretical Analysis

Figure 1 shows the geometric configuration of an acoustic source (Q) in a flow, the position of the velocity and temperature shear layer and the position of the receiver (M) in the surrounding medium at rest. The purpose of the theoretical analysis is to determine the acoustic pressure level at the point A (Figure 1) which is emanated under the true radiation angle, as related to the one measured at (M), as a function of suitable dimensionless influencing parameters. Therefore, we wish to find the following relationships:

$$(\varphi - \varphi_M) = \text{function}\,(\varphi_M,\ h/Y,\ M,\ t_i/t_a) \qquad (1)$$

$$P_A/P_M = \text{function}\,(\varphi_M,\ h/Y,\ M,\ t_i/t_a)\ . \qquad (2)$$

In order to determine the rotation of the wave front when passing through the separation layer between the moving and the rest medium, we use the Mach wave analogy shown in Figure 2, which is based on an analysis by Ribner [3]. The sound waves which impinge on the separation surface and come from the moving medium (i) produce a disturbance (ripple) in it, which propagates with a speed above the speed of sound. In the present case, this perturbation velocity is found as the sum of the velocity component parallel to the separation layer of the velocity triangle formed with the local speed of sound and the flow velocity U. /11

Similar to this representation, according to the discussion by Ribner, the perturbation can be considered to be fixed, and instead the medium can be considered to be moving with the perturbation velocity, but in the opposite direction. The acoustic wave reflected by the separation layer as well as the acoustic waves radiated into the medium at rest (a) can be interpreted as Mach waves produced by the fixed perturbation. From the velocity triangles shown in Figure 2, we then find the following relationship:

$$U_a = U_i + U \tag{3}$$

in other words

$$\frac{c_a}{\cos\varphi} = \frac{c_i}{\sin\alpha} + U \quad . \tag{4}$$

In dimensionless notation, equation (4) then becomes

$$\frac{1}{u\cos\varphi} = \frac{1}{\sin\alpha} + M \qquad \text{with} \quad u = \sqrt{t_i/t_a} \tag{5}$$

where M is the Mach number of the flow.

Using some geometrical analysis on the propagation of the wave fronts, in the flow, Amiet then finds the following relationship

$$\frac{\cos\alpha}{\sin\alpha+M} = \frac{h}{x_o} = \tan\varphi' \tag{6}$$

and

$$Y \cot\varphi_M = h \cot\varphi' + (Y - h) \cot\varphi \tag{7}$$

or

$$\tan\varphi_M = \frac{\tan\varphi' \tan\varphi}{(h/Y) \tan\varphi + [1-(h/Y)] \tan\varphi'}$$

From equations (5) and (6) one finally obtains the following relationship

$$\tan\varphi' = \frac{h}{x_o} = \frac{\zeta}{(1-M^2)\,\mu\cos\varphi + M} \tag{8}$$

with

$$\zeta = \sqrt{(1-M\,\mu\cos\varphi)^2 - \mu^2\cos^2\varphi} \tag{9}$$

Based on equations (7) and (8), by using an iteration one can find the desired relationship (equation (1)) for the angle of the source (Q) and receiver (M) (Figure 1) connection line and the true radiation angle. In order to determine the change in the pressure amplitude when a sound wave passes through the separation layer, Ribner [3] gives the transmission loss in the following form

$$\frac{P_{c-}}{P_{c+}} = \frac{1}{T} = \frac{1}{2} + \frac{\rho_i c_i^2 M^2 (M_a^2 - 1)^{0,5}}{2\rho_a c_a^2 M_a^2 (M^2 - 1)^{0,5}} \tag{10}$$

The pressure P_{c-} describes the amplitude of the acoustic

wave which impinges onto the separation surface of pressure P_{c+} of the transmitted wave. In the present case, the density difference between the medium at rest and the moving medium is only to be attributed to a temperature change by using /13

$$\frac{\rho_a c_a^2}{\rho_i c_i^2} = 1 \qquad (11)$$

It is found that an amplitude change is only indirectly dependent if there is a temperature shear layer, that is only through an angle change. Using equations (5), (9) and (11), and a few geometric relationships, equation (10) can be written in the form

$$\frac{P_{c-}}{P_{c+}} = \frac{1}{T} = \frac{1}{2\zeta}\left(\zeta + \sqrt{1-\mu^2\cos^2\varphi}\,(1-M\mu\cos\varphi)^2\right) \qquad (12)$$

In order to calculate the pressure amplitude at the position (A) in the medium at rest (Figure 1), we must now determine the divergence of the acoustic rays along the propagation path. According to the geometry shown in Figure 3, according to Amiet, we find the following for the propagation in the x-y plane

$$\frac{dl_2}{dl_1} = 1 + (Y-h)\,\frac{1}{\sin^2\varphi}\,\frac{d\varphi}{dx_o} \qquad (13)$$

By substitution

$$\left|\frac{dx_o}{d\varphi}\right| = \left|\frac{dx_o}{d\alpha}\,\frac{d\alpha}{d\varphi}\right| = \left|\frac{h(1+M\sin\alpha)}{\cos^2\alpha}\cdot\frac{(-\mu)\sin\varphi}{\zeta(1-M\mu\cos\varphi)}\right| = \left|\frac{-\mu h\sin\varphi}{\zeta^3}\right| \qquad (14)$$

in equation (13) one finally obtains

$$\frac{dl_2}{dl_1} = 1 + \left(\frac{Y}{h} - 1\right)\frac{\zeta^3}{\mu\sin^3\varphi} \qquad (15)$$

For the divergence in the z direction according to Amiet we find

$$\frac{dz_2}{dz_1} = 1 + (Y-h)\,\frac{1}{\sin\varphi}\,\frac{d\psi'}{dz_1} \qquad (16)$$

the angle ψ' is the solid angle of the acoustic ray with respect to the x-y plane (Figure 4). /14

For the boundary condition for equal phase of the incoming and transmitted acoustic wave in the separation layer, Amiet obtains the following relations

$$\left(\frac{dz}{d\psi}\right)_{\psi=0} = \frac{\cos\varphi}{(1-M\cos\varphi)}\,\frac{h}{(1-M^2)}\left(\sqrt{(1-M^2)+\left(\frac{x_o}{h}\right)^2} - M\frac{x_o}{h}\right) . \qquad (17)$$

If the ratio x_o/h is eliminated using equation (8), then from this we obtain

$$\left(\frac{dz}{d\psi}\right)_{\psi=0} = \frac{h\cos\varphi}{\zeta}\,\frac{(1-M\mu\cos\varphi)}{(1-M\cos\varphi)} . \qquad (18)$$

For small angles ψ we have $\psi' \cong \psi\cdot\sin\phi$ and $\phi \cong \pi/2-\varphi$, that is $\psi' \cong \psi\cdot\cos\varphi$. Therefore we find

$$\frac{dz}{d\psi'} = \frac{dz}{d\psi}\,\frac{d\psi}{d\psi'} = \frac{h}{\zeta}\,\frac{(1-M\mu\cos\varphi)}{(1-M\cos\varphi)} \qquad (19)$$

and equation (16) is given the form

$$\frac{dz_2}{dz_1} = 1 + \left(\frac{Y}{h}-1\right)\frac{\zeta}{\sin\varphi}\,\frac{(1-M\cos\varphi)}{(1-M\mu\cos\varphi)} . \qquad (20)$$

The ratio of the pressure amplitudes between the location of the separation layer and the measurement point can therefore now be determined as a consequence of the divergence of the sound rays, according to

$$\frac{P_{c+}}{P_{c-}} = \sqrt{\frac{dz_2}{dz_1}\,\frac{dl_2}{dl_1}} \qquad (21)$$

where P_{c+} is the acoustic pressure after passing through the separation layer. The ratio of the pressure amplitudes P_{c-}/P_{c+}, that is the pressure change when passing through the separation layer,was specified by equation (12). Therefore, /15 we have the following for the desired ratio of the pressure amplitude at the point A and the pressure amplitude at the point (M)

$$\frac{P_A}{P_M} = \frac{P_{c+}}{P_M}\cdot\frac{P_{c-}}{P_{c+}}\cdot\frac{P_A}{P_{c-}} = \frac{P_{c+}}{P_M}\cdot\frac{P_{c-}}{P_{c+}}\cdot\frac{h}{Y} \qquad (22)$$

Using equations (12) and (21) we finally obtain the desired correction equation for the acoustic pressure amplitude in the desired dimensionless form

$$\frac{P_A}{P_M} = \frac{h/Y}{2\,\zeta\sin^2\varphi}\left(\zeta + \sqrt{1-\mu^2\cos^2\varphi}\cdot(1-M\,\mu\cos\varphi)^2\right)$$
$$\cdot\sqrt{\left(\sin\varphi + \left(\frac{Y}{h}-1\right)\zeta\,\frac{(1-M\cos\varphi)}{(1-M\,\mu\cos\varphi)}\right)\left(\sin^3\varphi + \left(\frac{Y}{h}-1\right)\frac{\zeta^3}{\mu}\right)} \qquad (23)$$

In the case of equal temperature in the flow and in the surrounding medium, the temperature ratio takes on the value of 1, and the correction equations (7), (8), (9) and (23) then are given the form specified by Amiet [1].

2.2 Discussion of Results

Figures 5, 6 and 7 show calculation results of the shear layer correction for selected values of the dimensionless influence parameters. That is, the geometric ratio h/Y, the

temperature ratio, t_i/t_a and the flow Mach number M. In order to show the substantial important trends for the deviations referred to the measurement point (M) as well as that of the true radiation angle and the corresponding acoustic pressure level, first we assume two limiting values for the geometric ratio h/Y.

Figure 5 shows the correction quantities as a function of the geometric propagation angle φ_M to the measurement point for the ratio $h/Y \to 0$, . This is for a measurement location whose distance from the source is substantially greater than the lateral dimensions of the flow field in which the source is located. For the case of equal temperature in the flow and in the surrounding medium at rest, we then obtain the correction values which are well known from the literature: the true radiation angle from the source is always smaller than the geometric angle between the measurment point. The magnitude of the angular difference increases with increasing flow Mach number. In addition, in the range of small angles, we have the phenomena of total reflection at the shear layer, i.e., the sound radiated by the source against the flow direction is "captured" in the flow (for example, at M = 0.3 for $\varphi_M < 40°$)). The condition for the occurrence of total reflection according to equations (8) and (9) is the following

/16

$$\varphi < \arccos\left(\frac{1}{\mu(1+M)}\right) \qquad (24)$$

because of $\varphi' = 0$ in equation (8).

Regarding the correction of the acoustic pressure level determined at the measurement point (M) it is found that in the considered angular range, when recalculating the level values to the geometric location (A) of the intersection point between a ray with the true radiation angle and a line parallel to the flow direction through the measurement point at angles

of $\varphi_M > 90°$, the sound pressure levels are greater. On the other hand, below 90° they are smaller. With increasing flow Mach number, the magnitude of the level difference to be corrected increases.

From these results, we find that nothing changes when one assumes a temperature difference between the medium at rest and the medium in motion. It is only due to a corresponding change in the angular correction that there is also a change in the correction of the pressure amplitudes.

For smaller Mach numbers and a relatively larger temperature change in the flow (in Figure 6: $m = 0.05$; $t_i/t_a = 1.5$) however there is a special feature for large radiation angles: the angular correction here becomes negative and therefore the sign in the level difference is reversed in this angular range, where otherwise it is positive. The reason for this is the fact that /17 for angles $\varphi_M > 90°$, the rotation of the wave fronts caused by the temperature jump compared with the rotation caused by the flow separation layer has the opposite sense, and can dominate for correspondingly lower flow Mach numbers.

The correction values shown in figure 6 apply for a ratio of $h/Y = 0.8$, that is for a measurement location, which is close to the shear layer compared to the distance of the sound source. The magnitude of the correction quantities varies as a function of the measured radiation angle caused by the resulting geometric differences. However, from this there is no principlal change with regard to the previously described relationships. However, it is remarkable, that at high flow Mach numbers there is a great influence of the temperature ratio on the correction of the pressure amplitude.

Figure 7 finally shows the influence of different temperature in the flow and the surrounding medium at rest for parameter values which can be considered typical for

noise measurements in low speed wind tunnels. It becomes clear that the temperature influence as a rule will only become effective at large measurement angles.

3. Representation of the Correction Parameters in a Nomogram

Figures 8 to 44 show the correction parameters - amplitude correction and angle correction - for selected parameter ranges in the form of nomograms. The temperature ratio t_i/t_a varies between 1.0 and 1.15 and the geometric ratio h/Y varies in the range 0 to 0.8. In each of these correction diagrams, the flow Mach number occurs as a parameter and passes through values between 0.05 and 0.3.

4. Summary

/18

Starting with the basic equations of Ribner and Amiet for the correction of acoustic signals after passing through a flow shear layer, we have determined the additional influence of different temperatures on both sides of the shear layer on the correction parameters. It is found that especially for large radiation angles compared with the flow direction, the influence of different temperatures in the flow and in the surrounding medium at rest must be considered for an accurate amplitude and angle correction.

For the parameter range which can be considered typical for noise measurements in free jet wind tunnels, we have calculated the correction parameters and have systematically compiled the calculated results in the form of nomograms.

5. References

[1] Amiet, R. K.
Correction of Open Jet Wind Tunnel Measurements for Shear Layer Refraction.
AIAA Paper No. 75-532, Hampton, VA./March 24-26, 1975.

[2] Herkes, W. H.
Strout, F. G.
Ross, R.
van Ditzhuizen, J.C.A.
Acoustic Evaluation of DNW Shear Layer Correction Using a Model Jet.
DNW TR 82.04, 1982.

[3] Ribner, H. S.
Reflection, Transmission and Amplification of Sound by a Moving Medium.
J. of the Acoustical Soc. of Am., Vol. 29, No. 4, pp. 435-441, 1956.

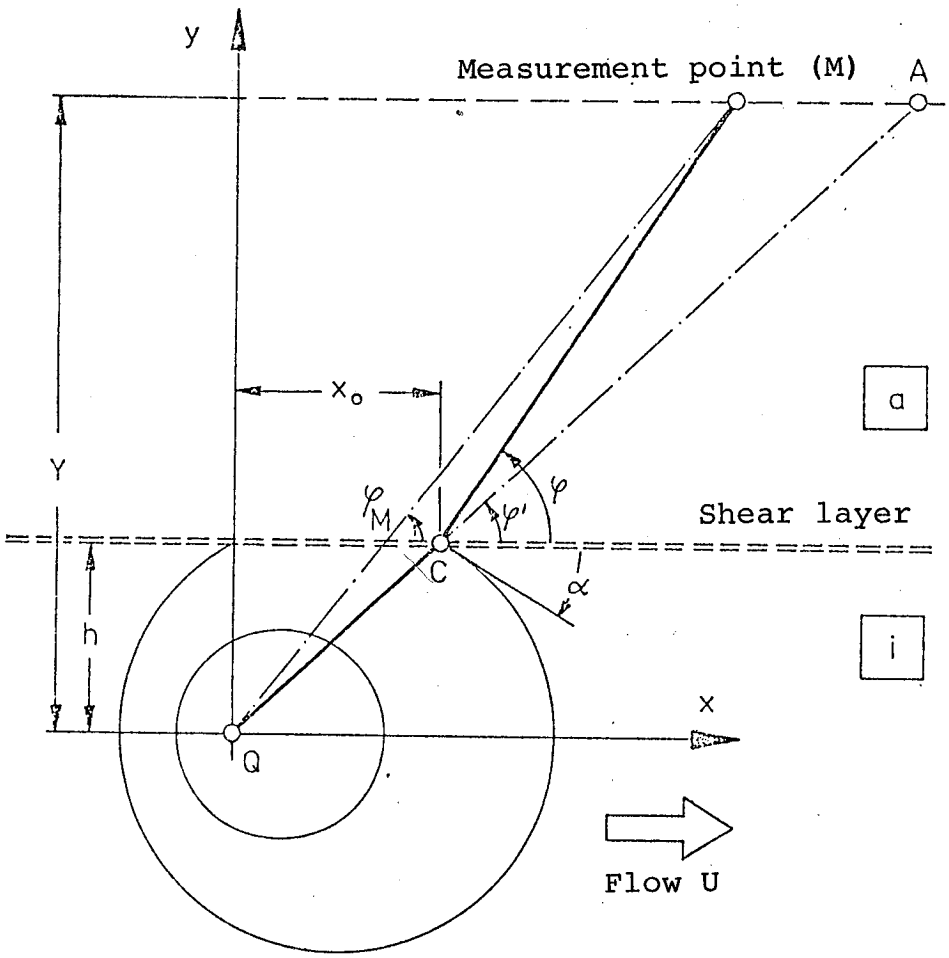

Figure 1. Geometric relationships when sound passes through a shear layer according to Amiet [1].

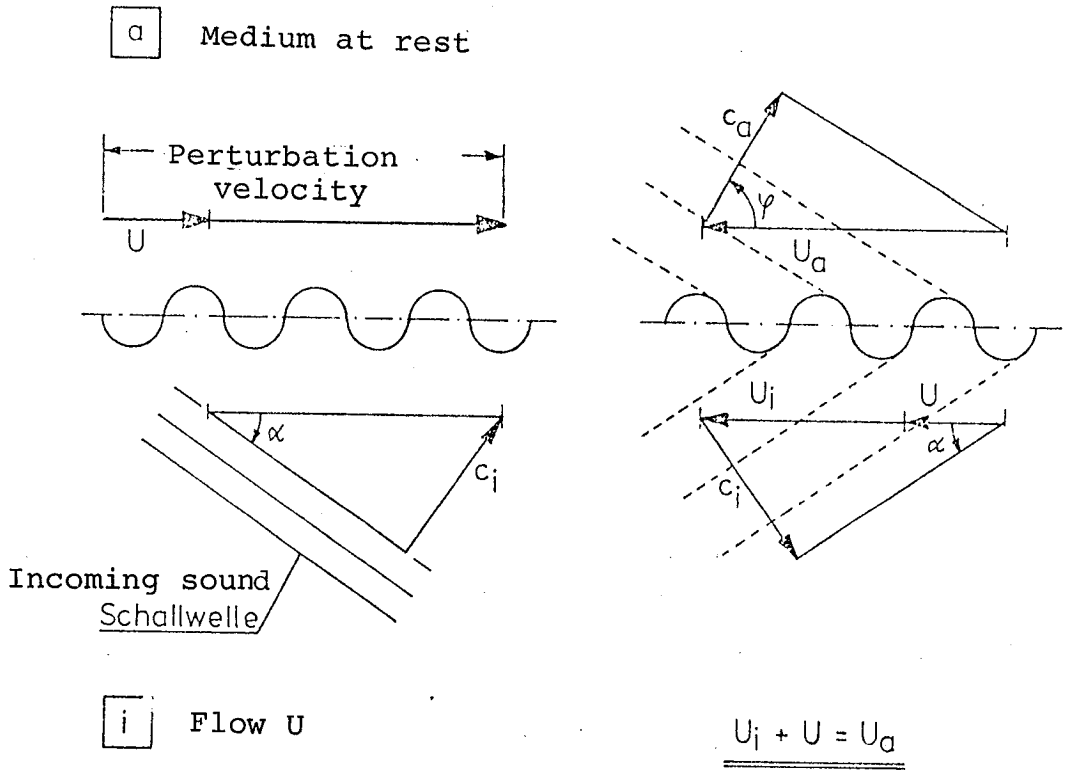

Figure 2. Sound propagation and reflection through and at a separation layer between a moving and a medium at rest according to Ribner [3].

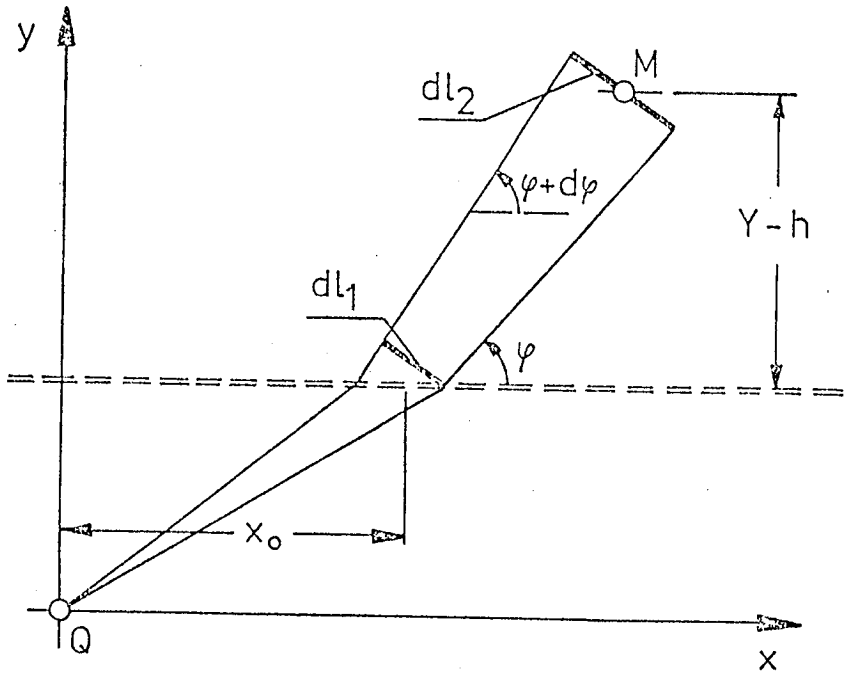

Figure 3. Sound propagation in the x-y plane.

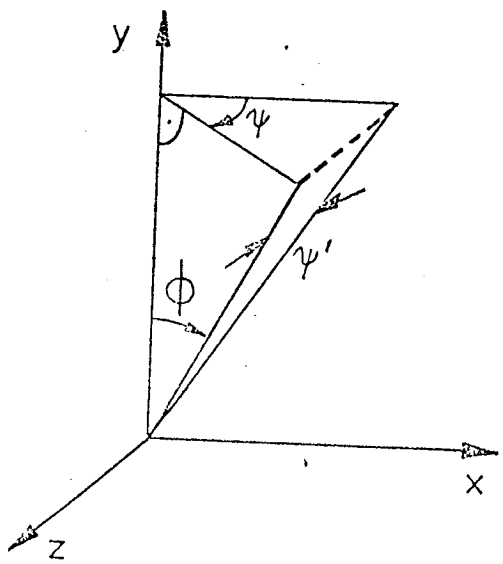

Figure 4. Angle definition for determining the sound propagation in the z direction.

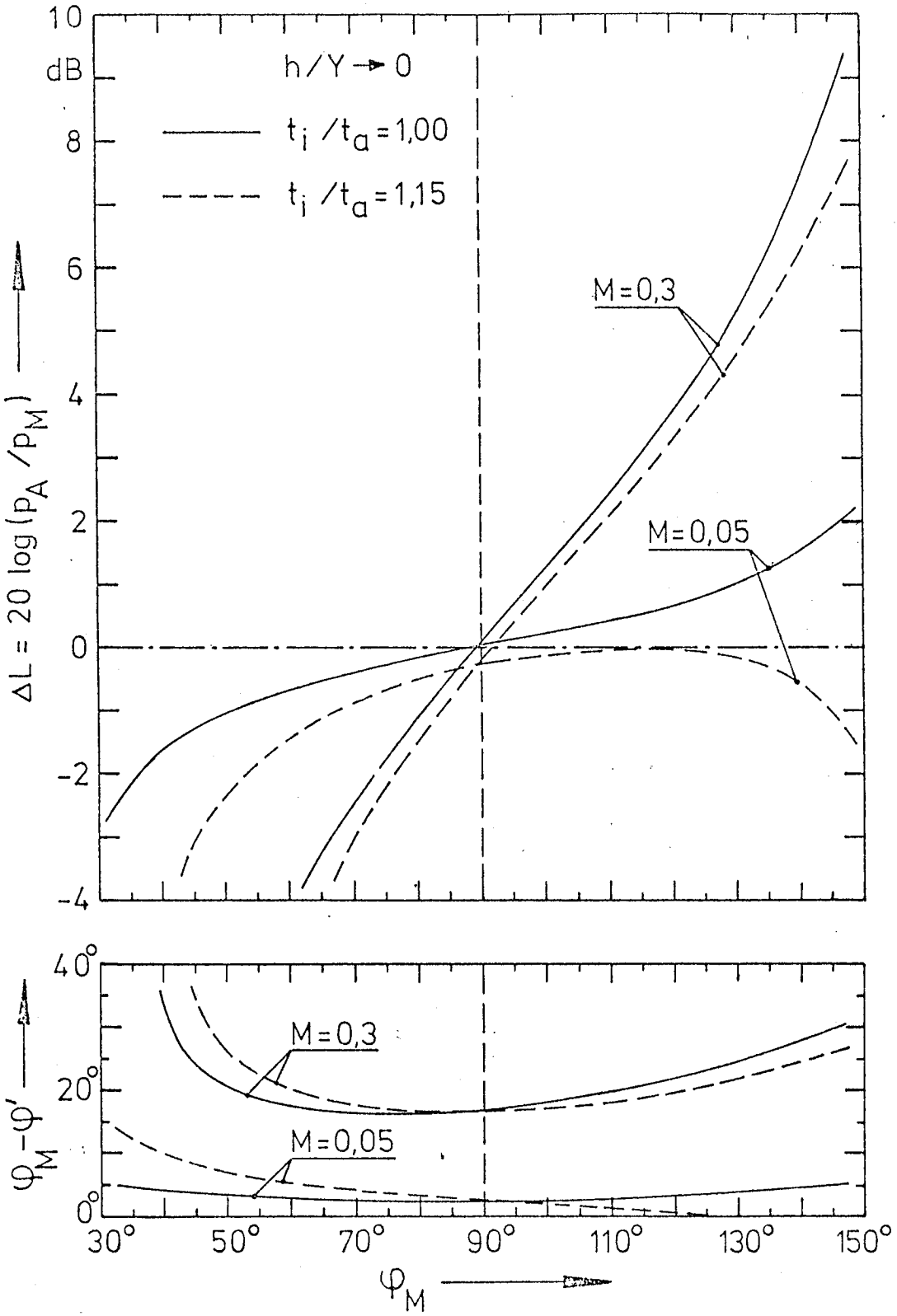

Figure 5. Influence of the flow Mach number and the temperature ratio on the amplitude and angle corrections for the ratio h/Y = 0 (large distance to the shear layer).

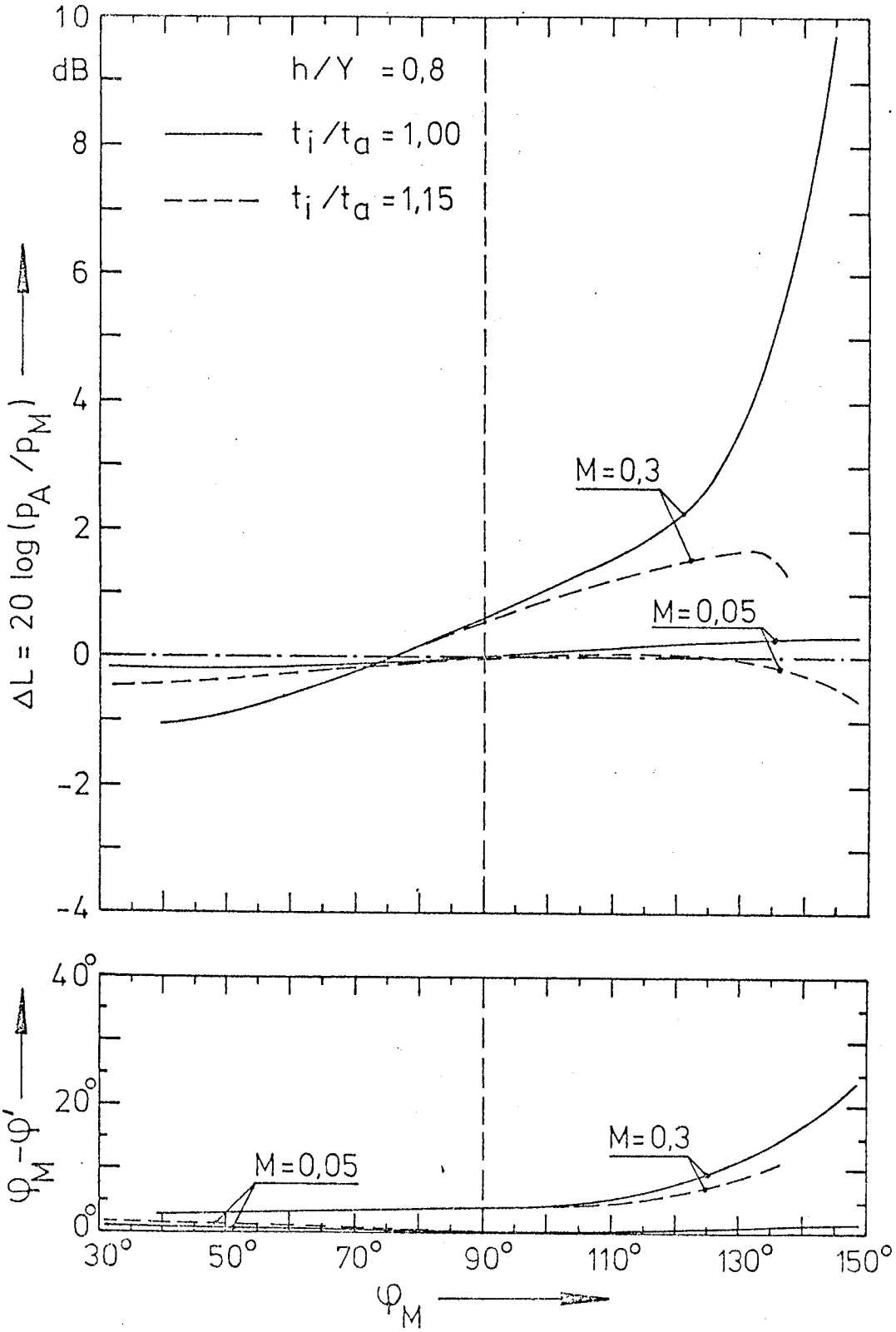

Figure 6. Influence of the flow Mach number and temperature ratio on the amplitude and angle corrections for the ratio h/Y = 0.8 (small measurement distance to the shear layer).

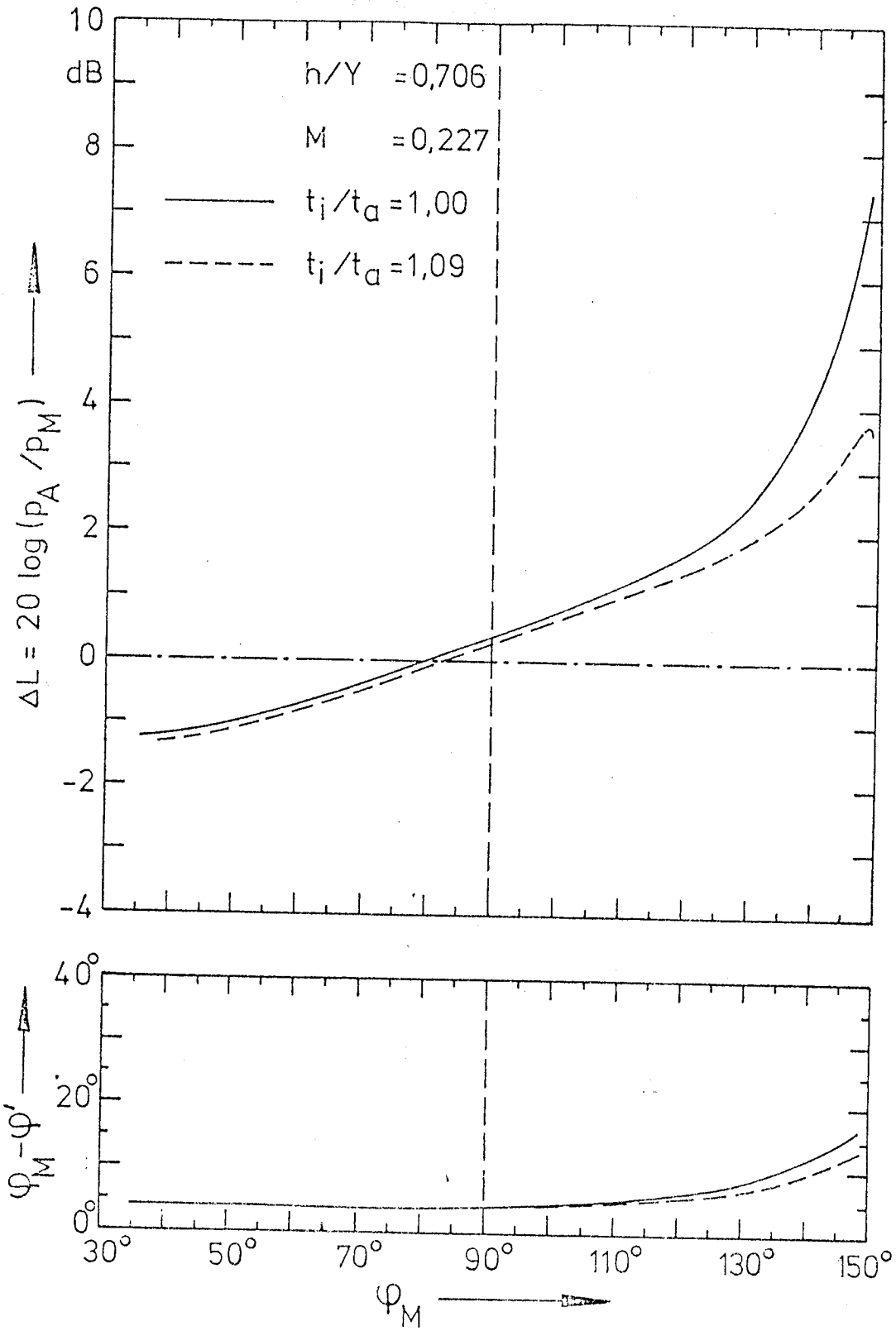

Figure 7. Determination of an amplitude and angle correction for typical measurement conditions in low speed wind tunnels.

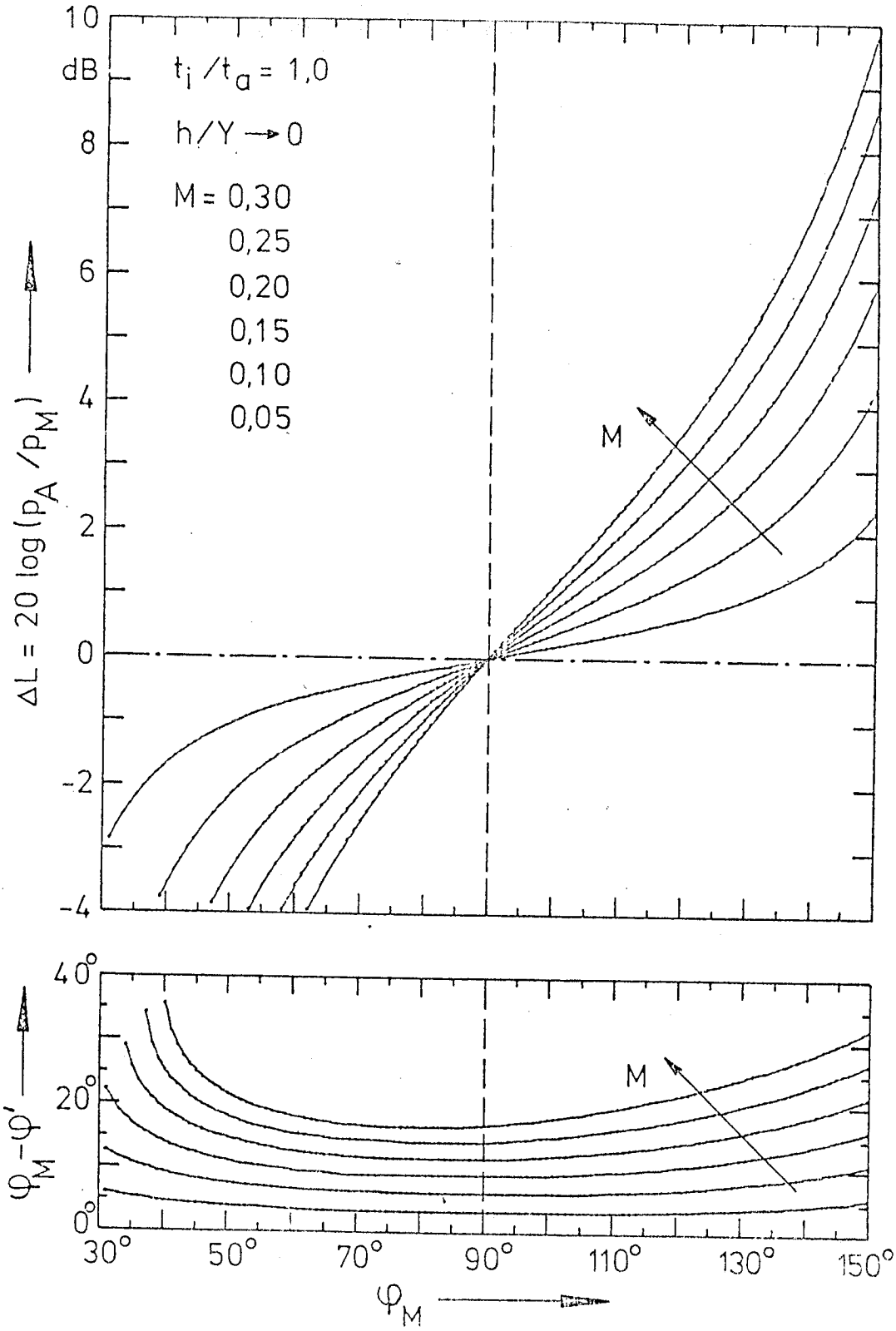

Figure 8. Amplitude and angle correction for different flow Mach numbers for $t_i/t_a = 1,0$; $h/Y \rightarrow 0$.

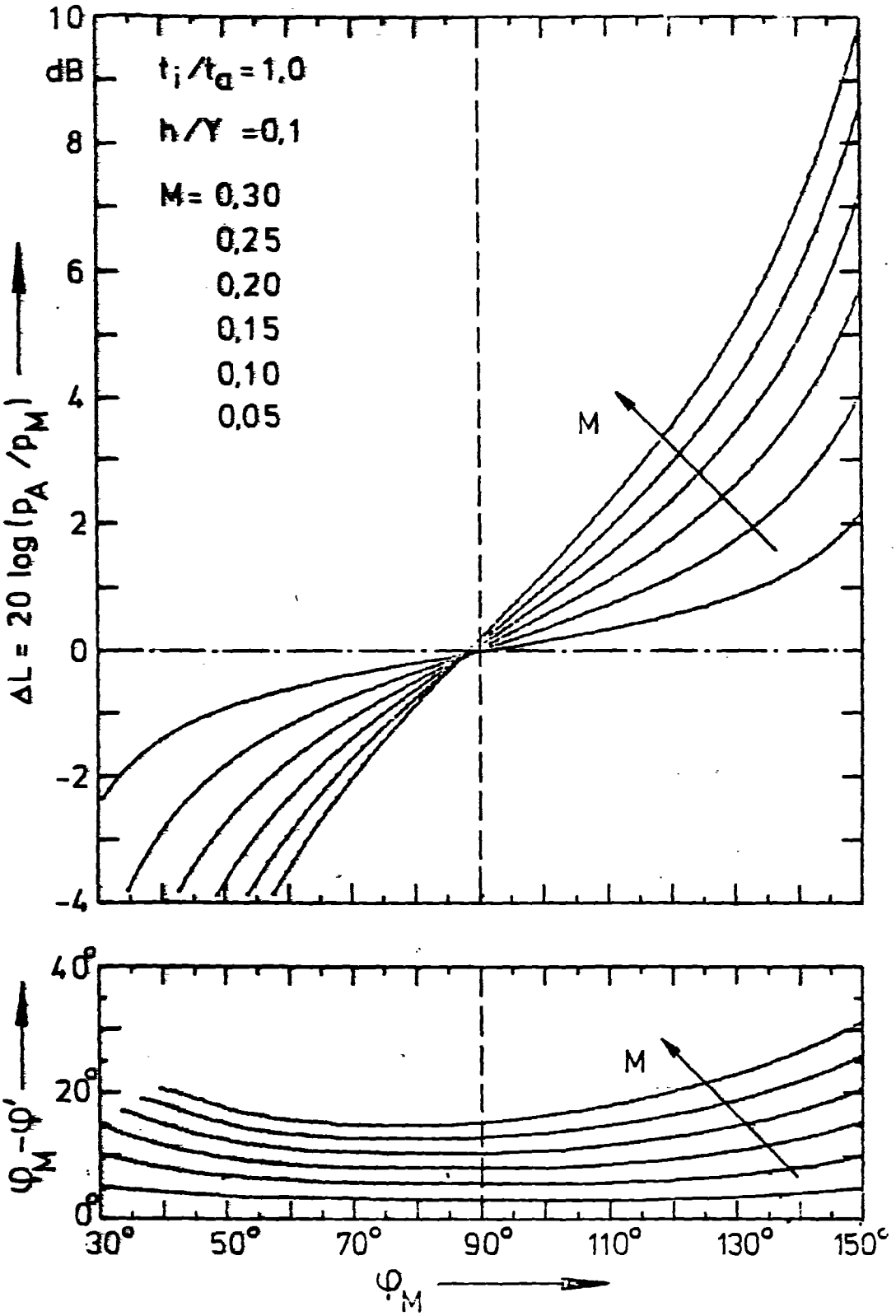

Figure 9. [illegible] at flow each [illegible] for $t_i/t_a = 1,0$; $h/Y = 0,1$.

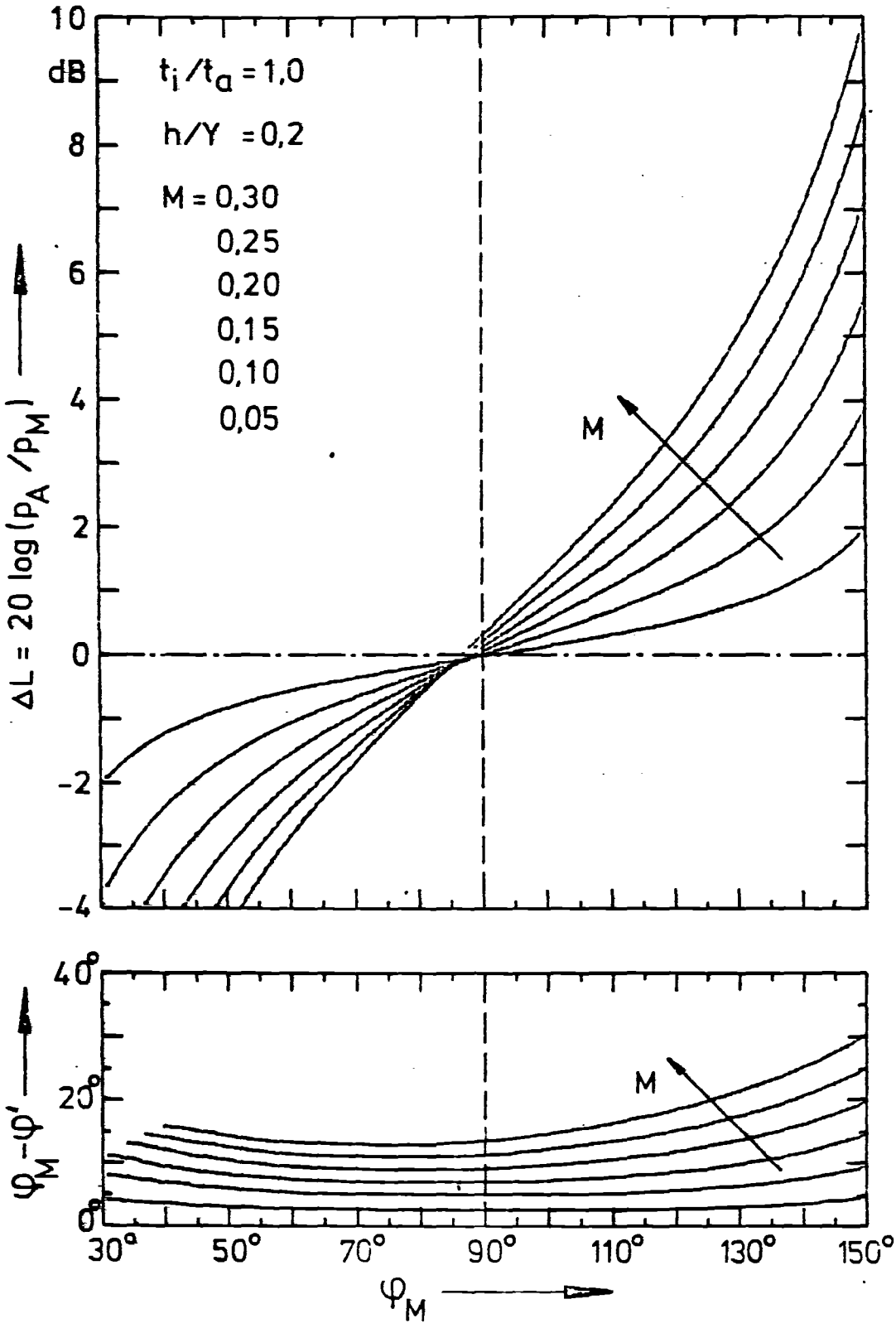

Figure 10. [illegible] for different flow mach numbers for t_i/t_a=1,0 ; h/Y=0,2

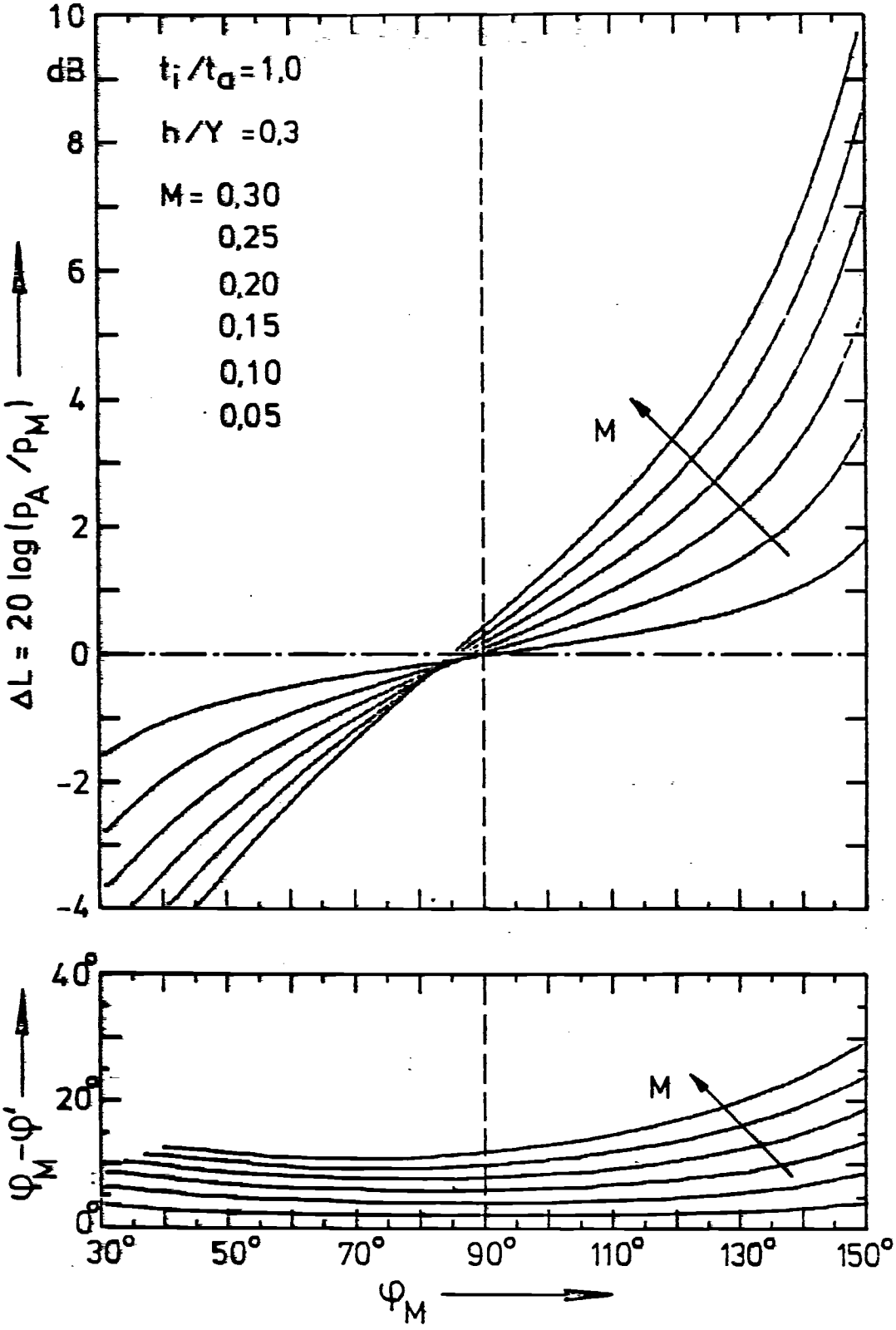

Fig. 11. [illegible] with

t_i/t_a=1,0 ; h/Y=0,3

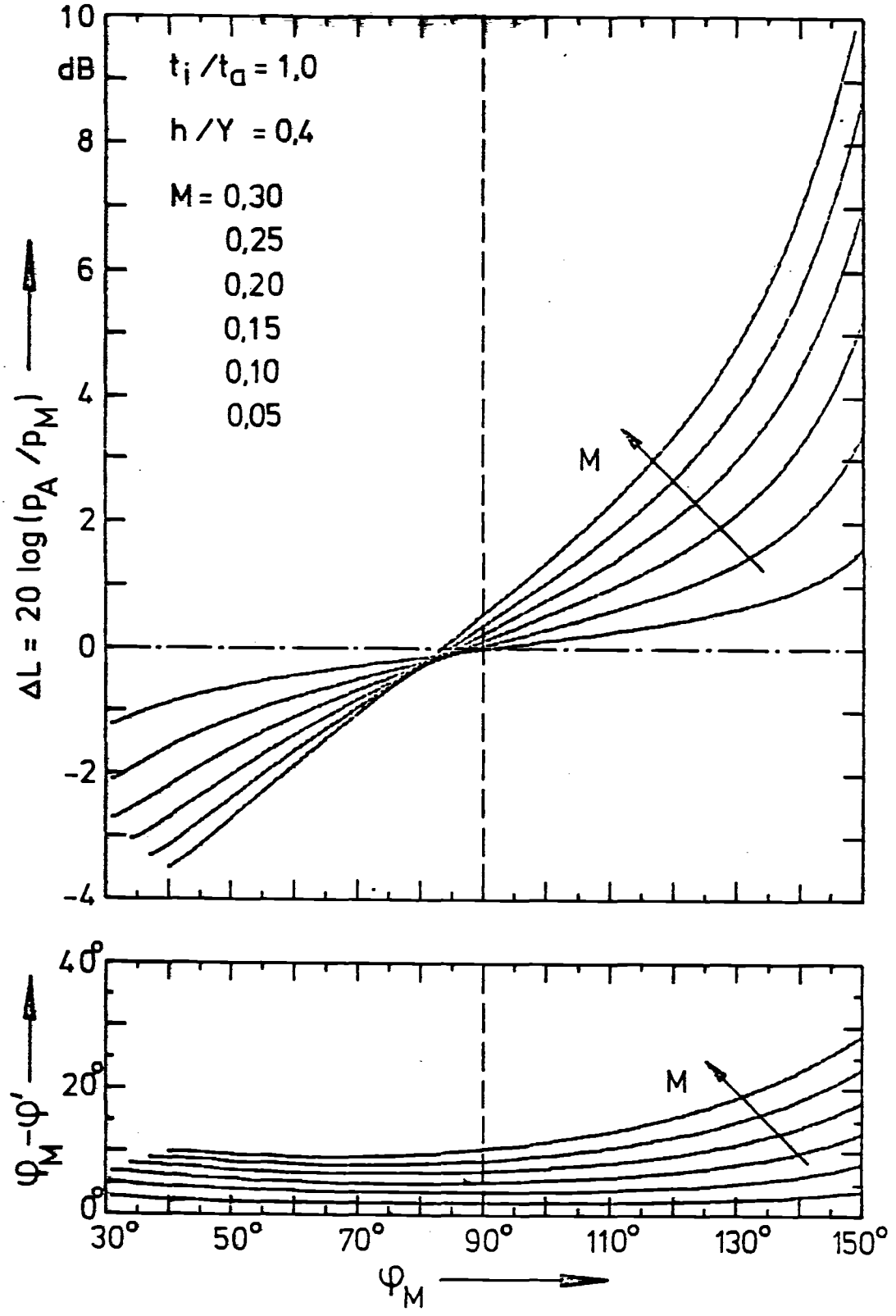

Figure 12. Amplitude and [illegible] with Mach numbers for $t_i/t_a = 1,0$; $h/Y = 0,4$

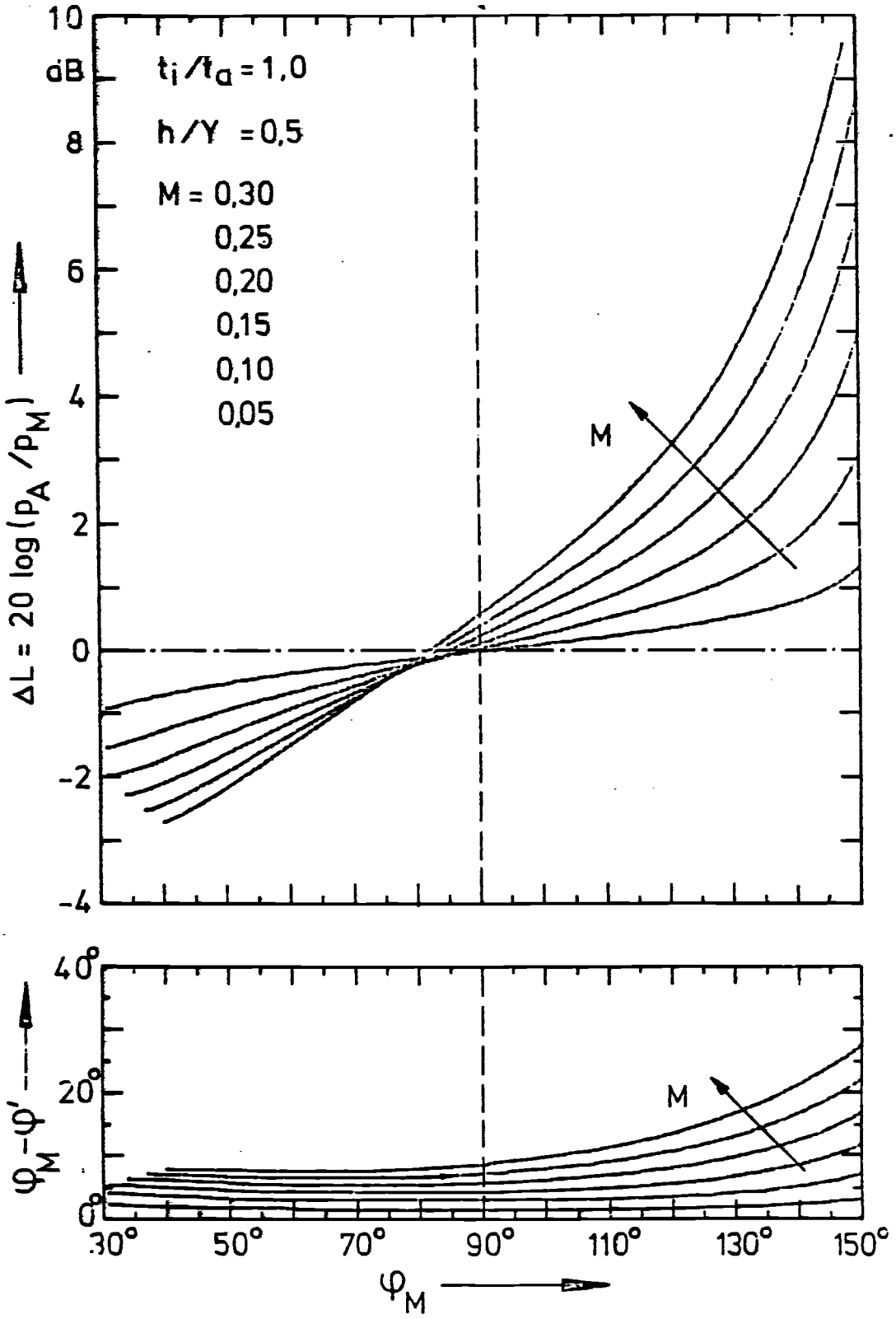

Figure 13. [illegible] and angle correction for [illegible] $t_i/t_a = 1,0$; $h/Y = 0,5$.

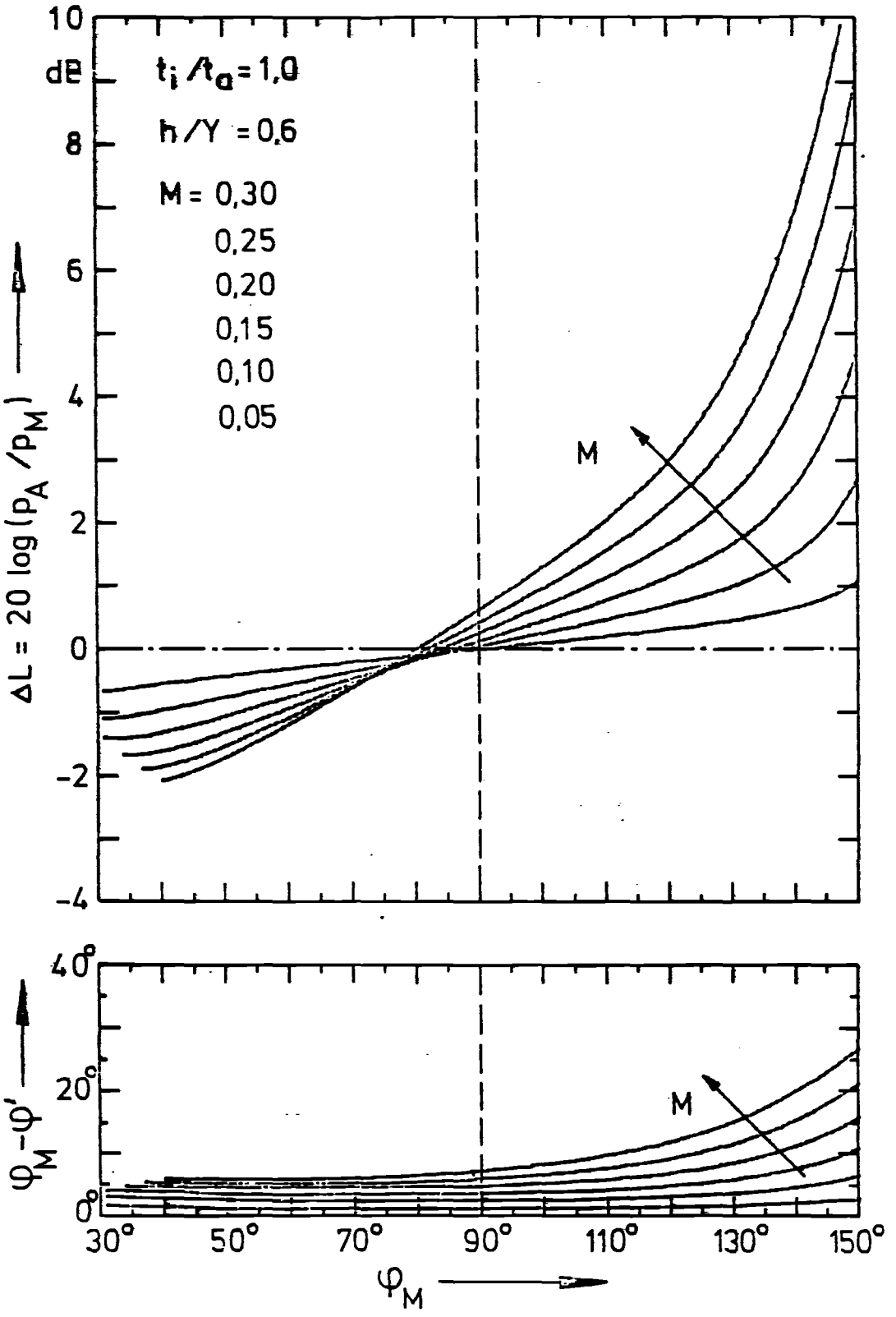

Figure 14. Amplitude and angle correction for different flow Mach numbers for $t_i/t_a = 1,0$; h/Y=0,6

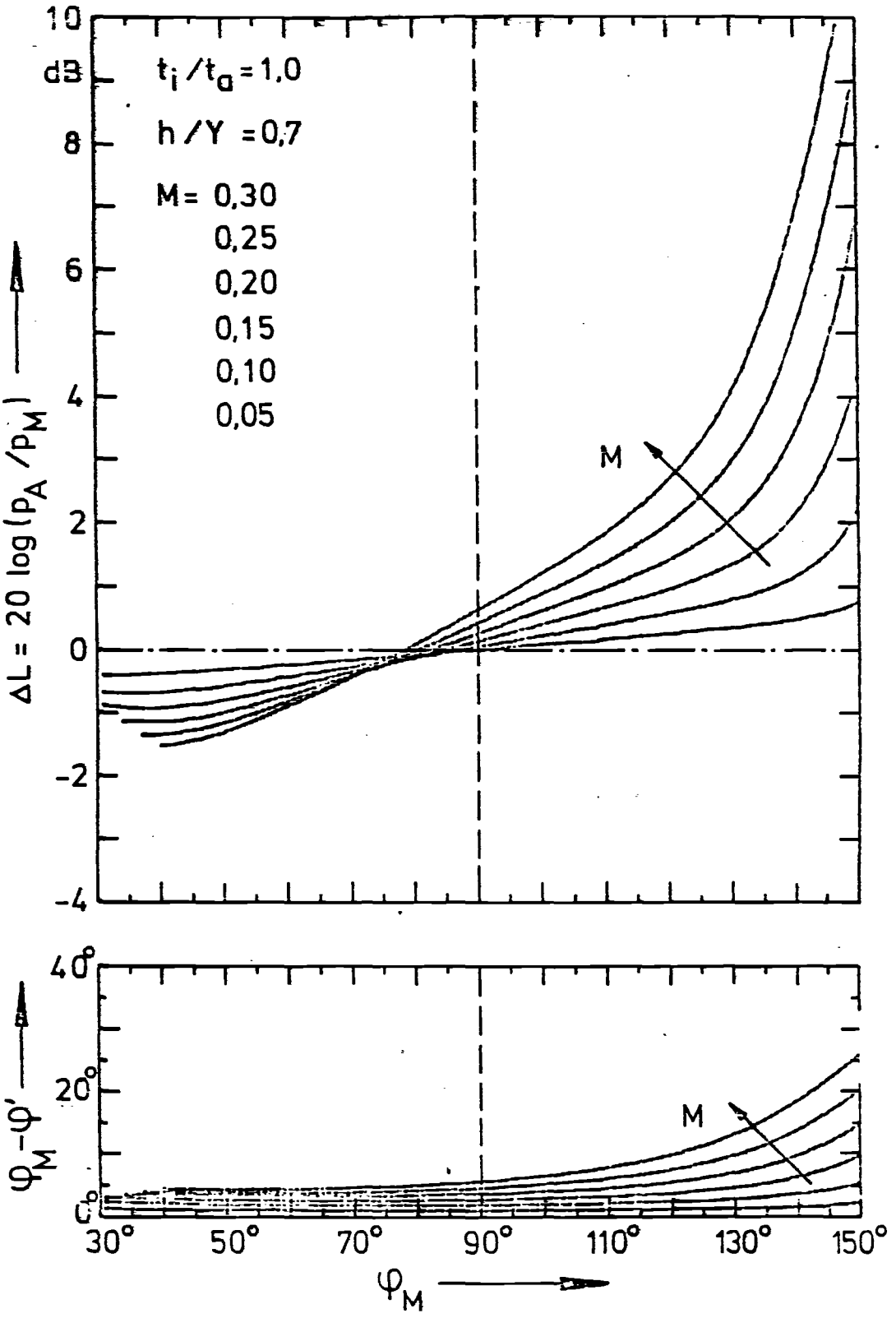

15.

$t_i/t_a = 1,0$; $h/Y = 0,7$

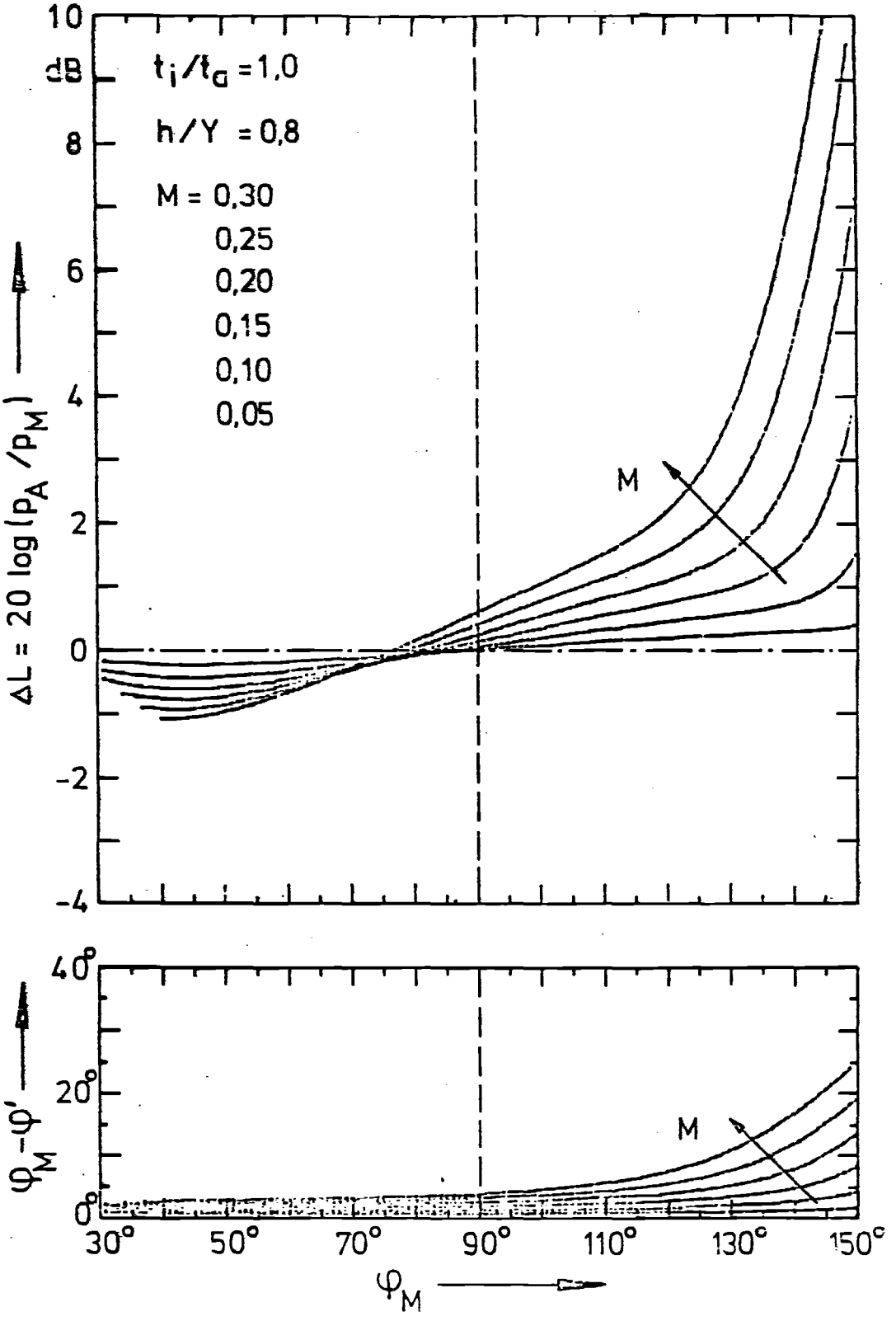

Fig. 16. [illegible] flow with $t_i/t_a = 1,0$; $h/Y = 0,8$

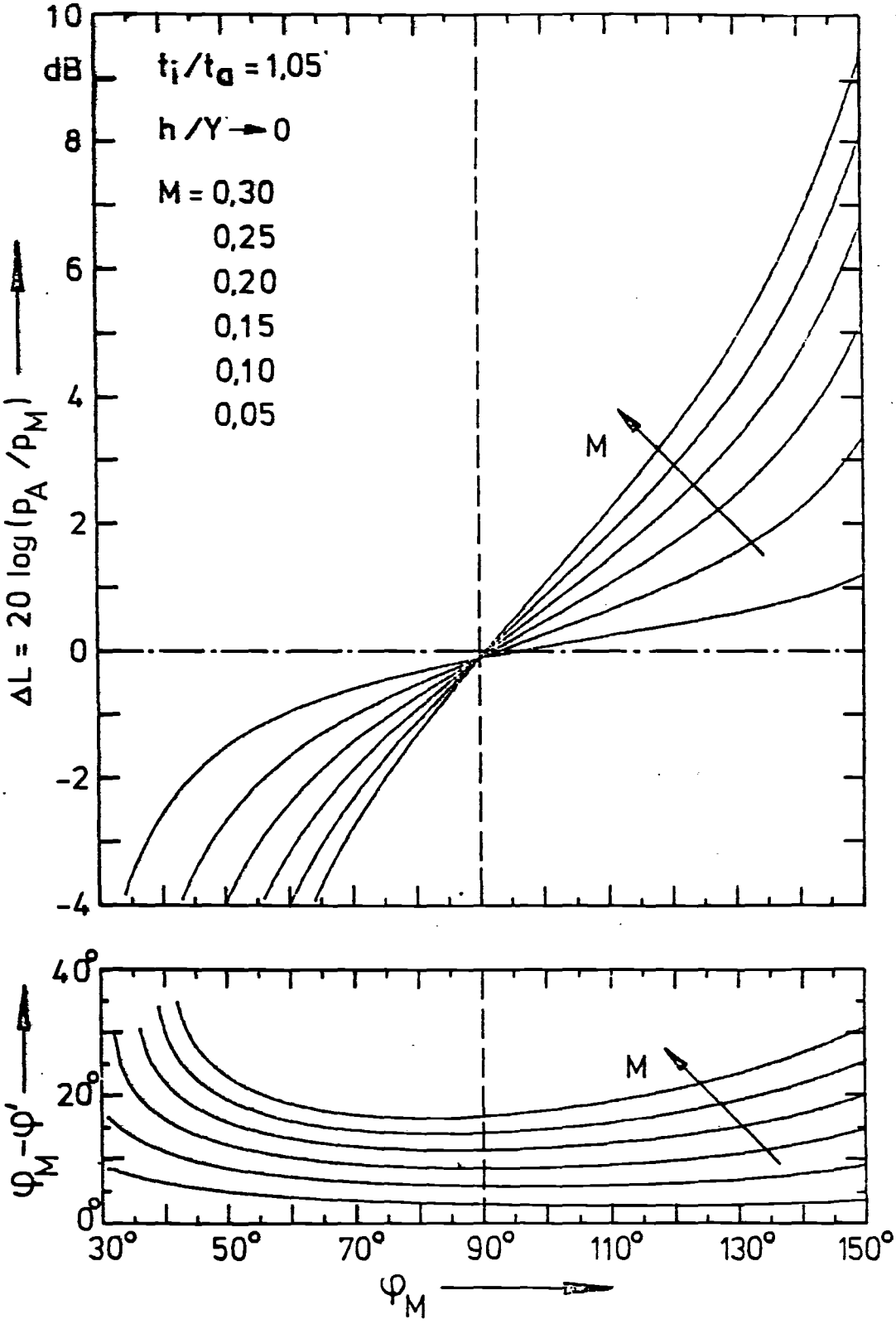

Figure 17. [illegible] and angle correction for different flow [illegible]
$t_i/t_a = 1{,}05$; $h/Y \to 0$.

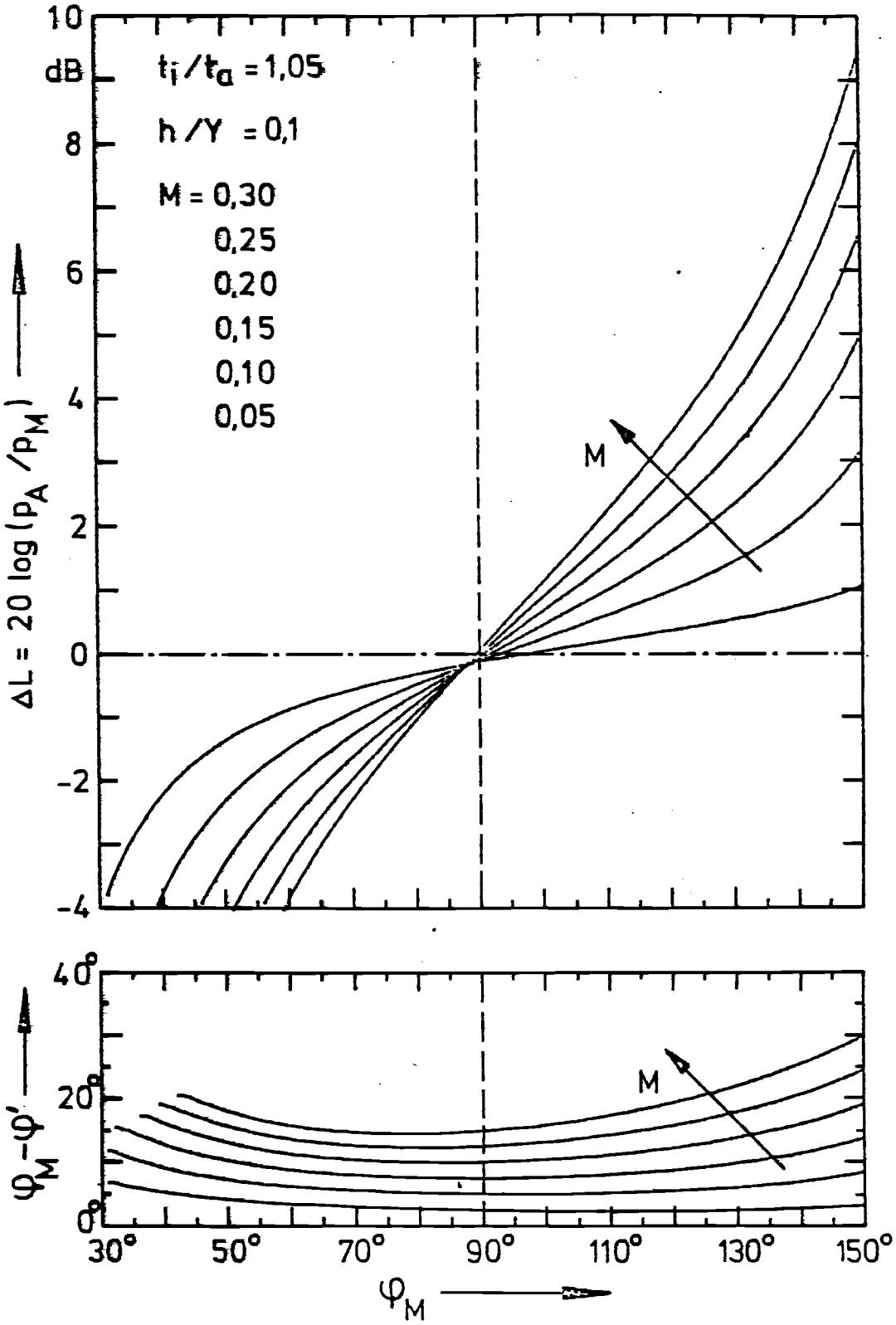

Figure 18. Amplitude and angle correction for different flow mach numbers for $t_i/t_a = 1,05$; $h/Y = 0,1$.

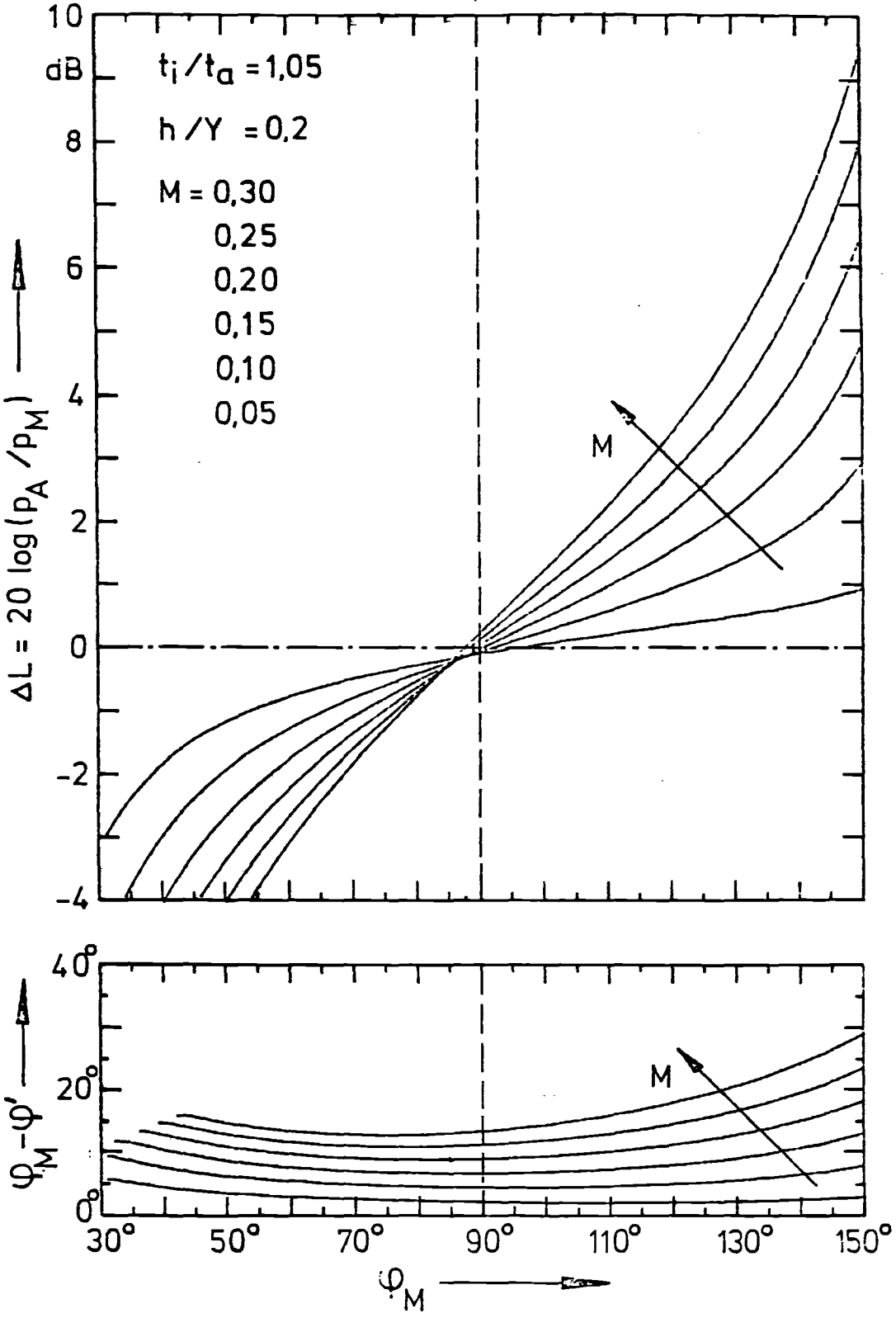

Figure 19. [illegible] t_i/t_a=1,05 ; h/Y=0,2

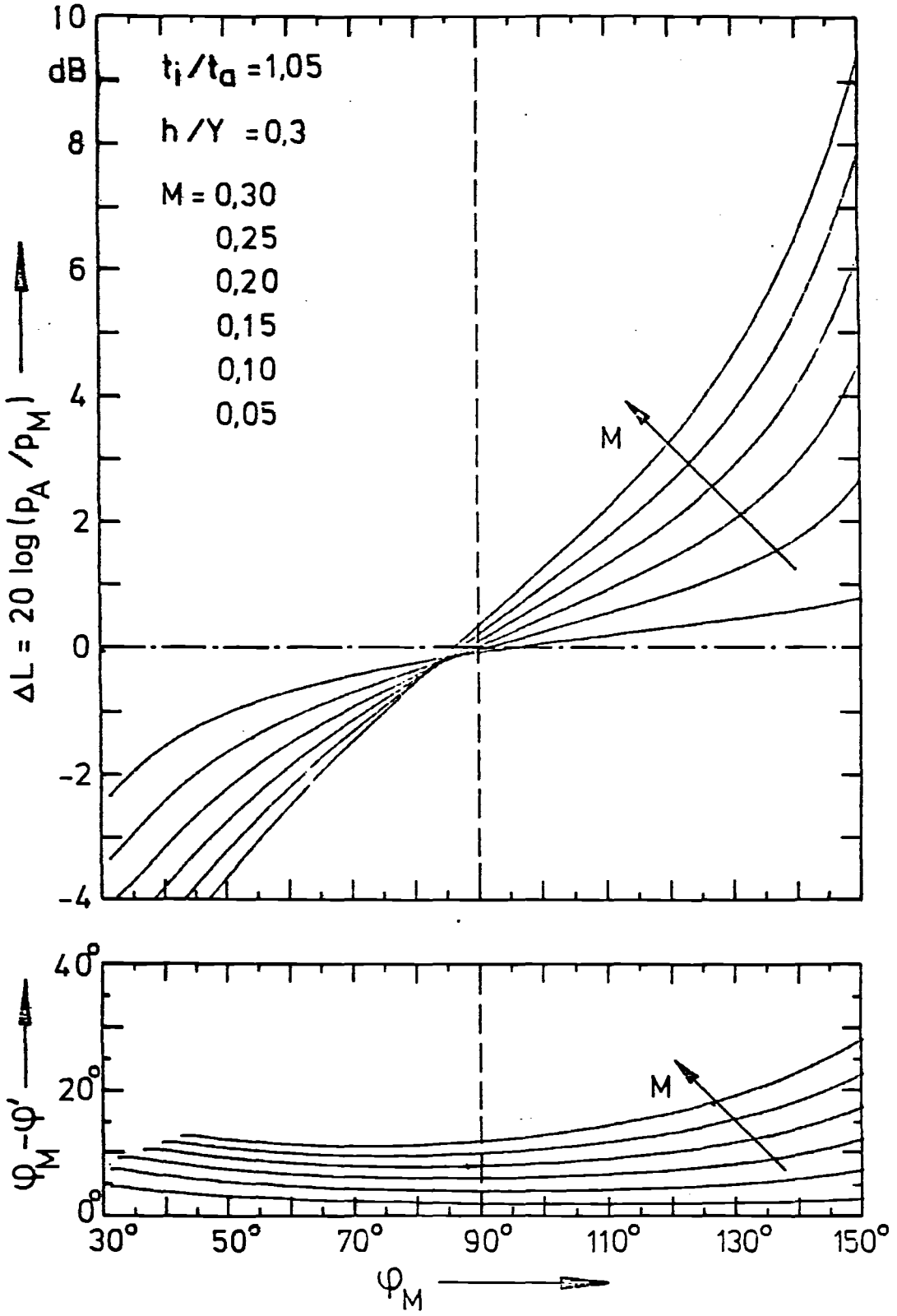

Figure 20. Amplitude and angle correction for different flow mach numbers for t_i/t_a=1,05 ; h/Y=0,3 .

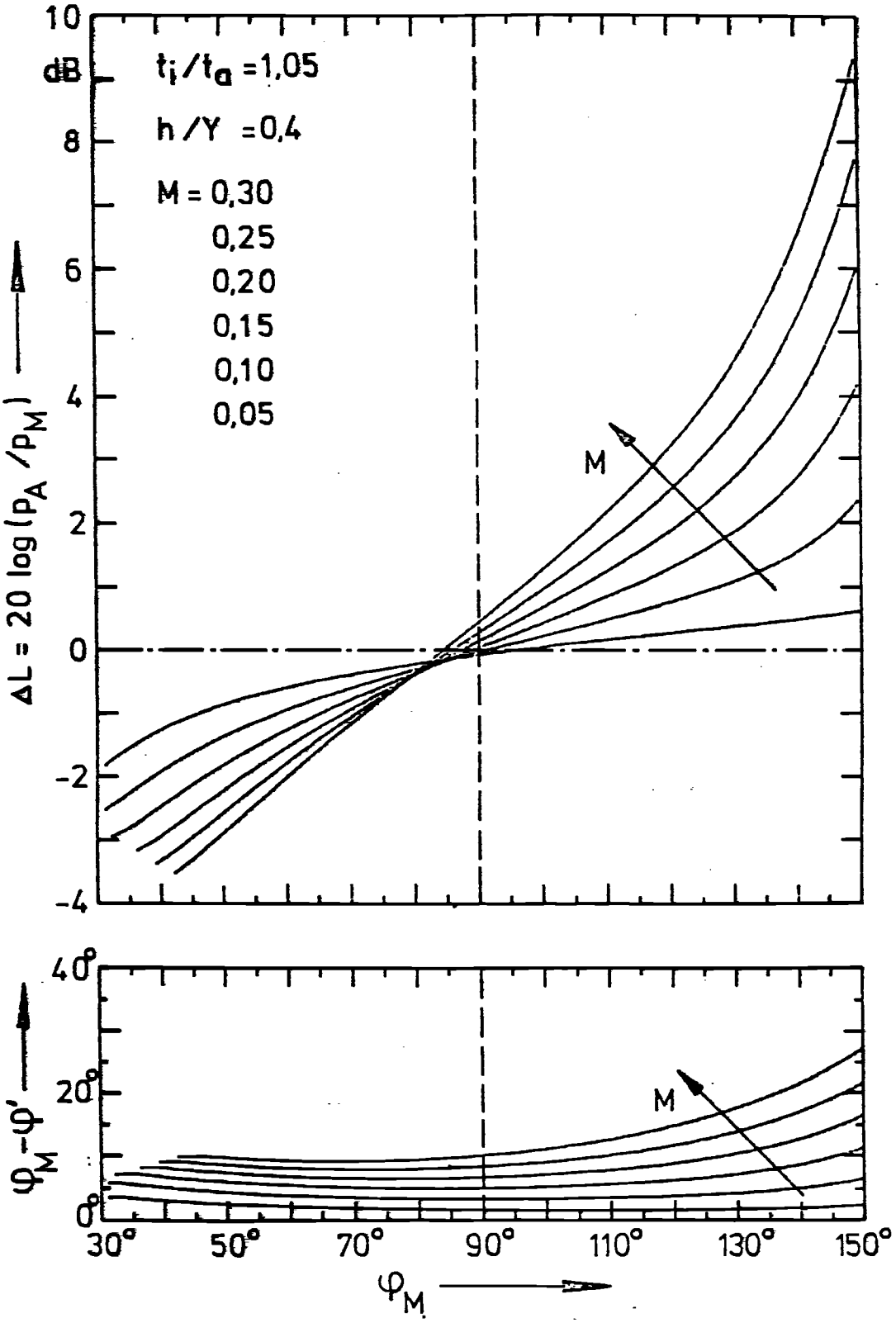

Figure 21. Amplitude and angle correction for different flow mach numbers for t_i/t_a=1,05 ; h/Y=0,4 .

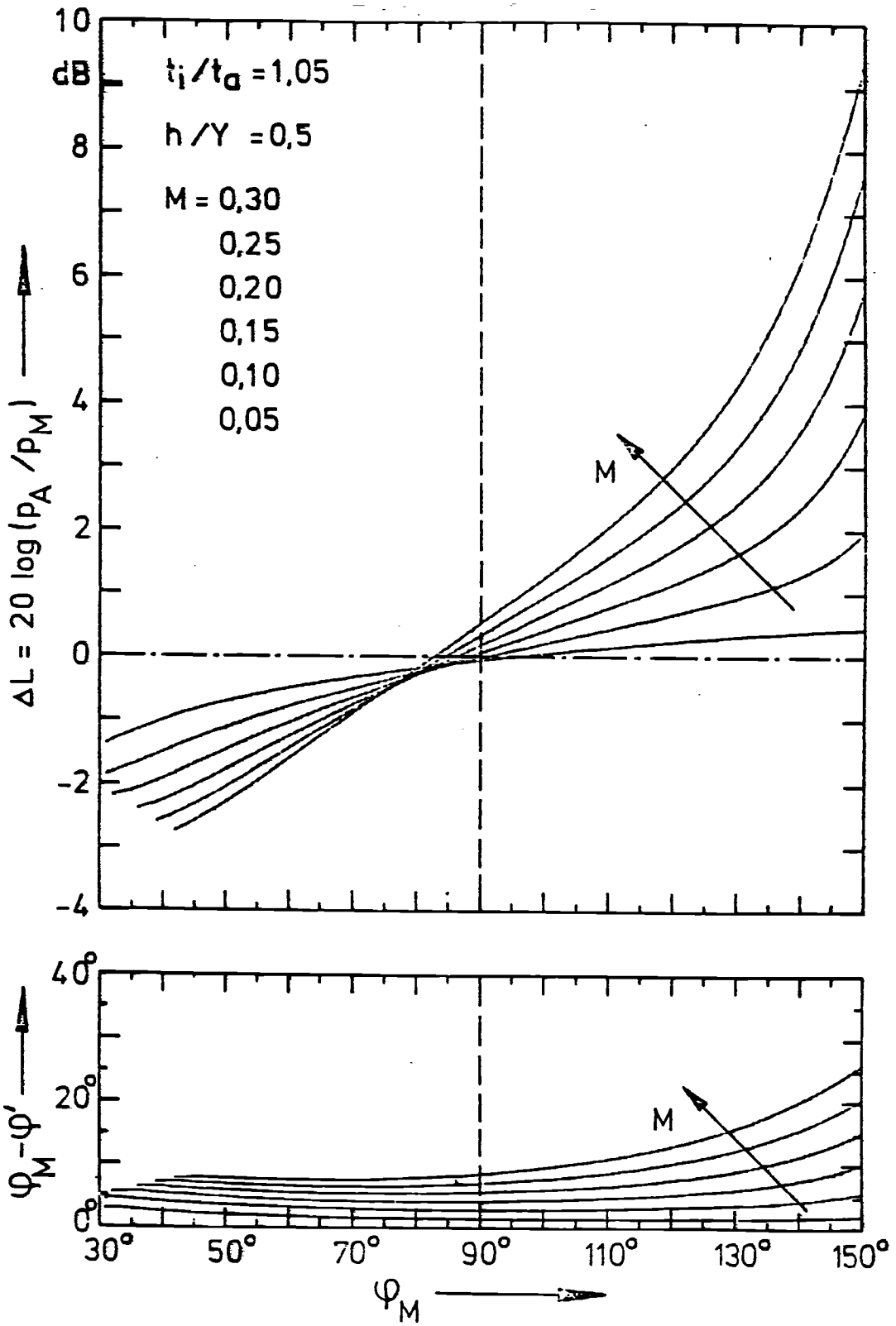

Figure 22. [illegible] correction for different flow mach [illegible] t_i/t_a=1,05 ; h/Y=0,5 .

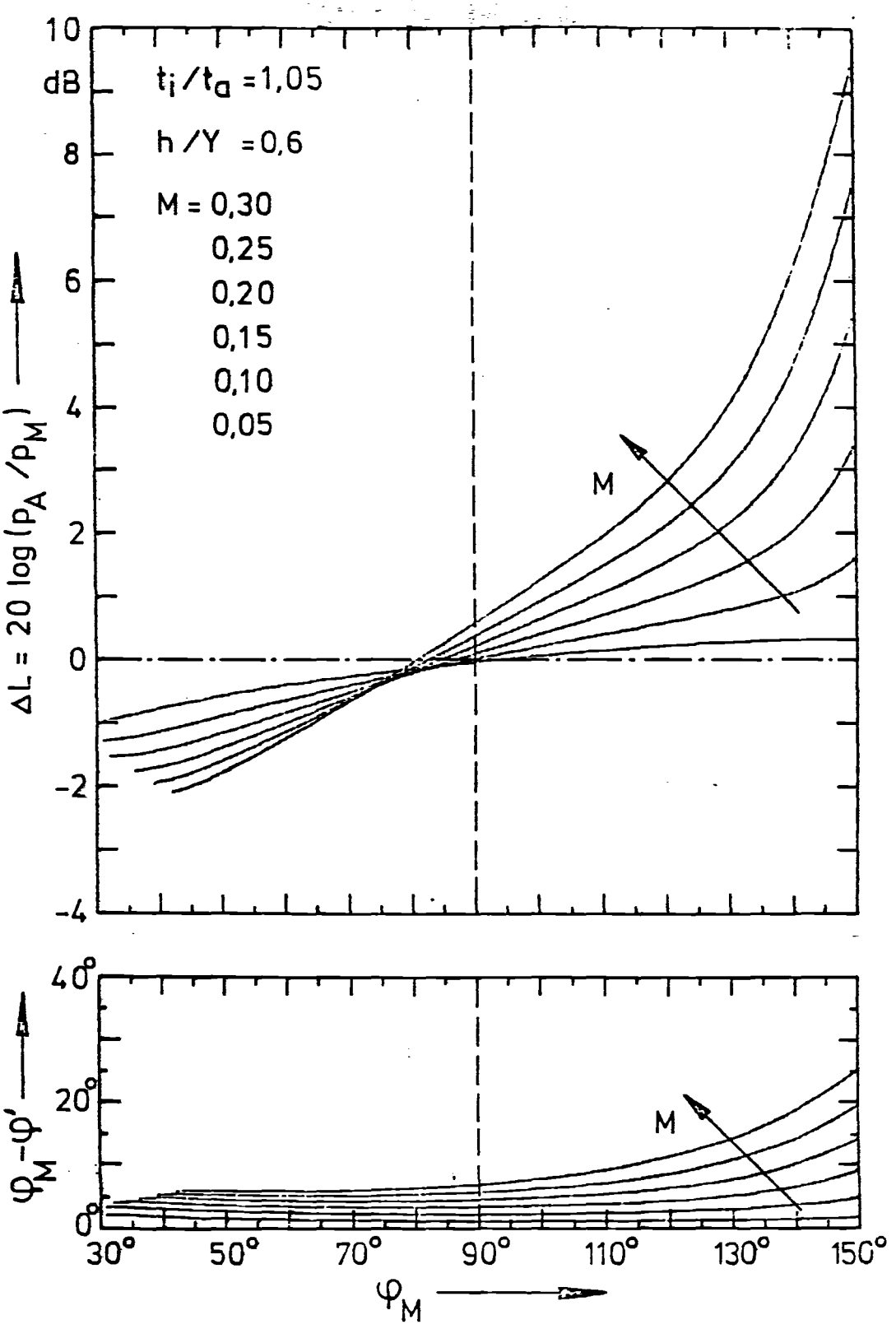

Figure 23. [illegible] tion for different flow Mach [illegible] t_i/t_a=1,05 ; h/Y=0,6 .

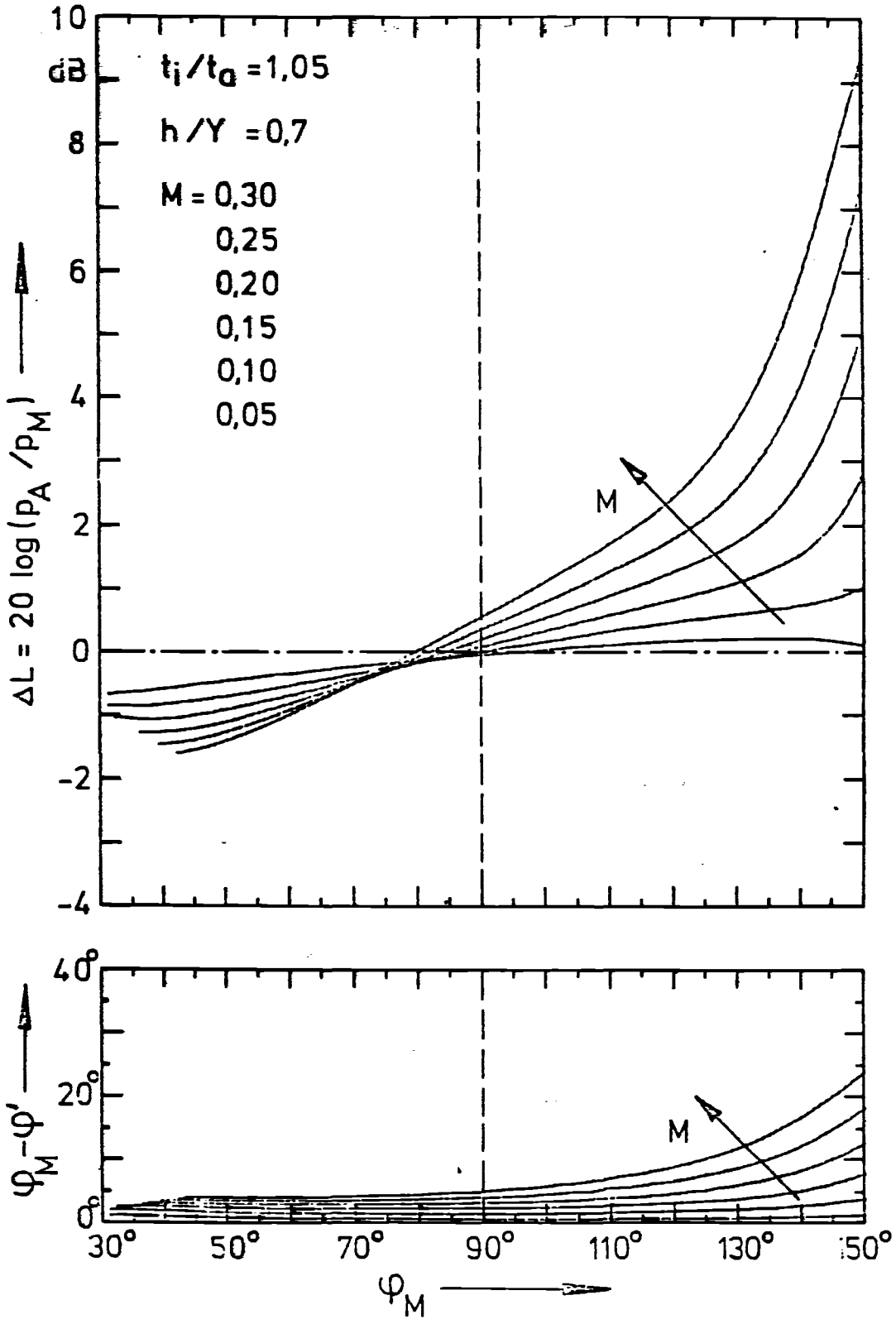

Figure 24. Amplitude and phase deviation for different flow mach numbers for t_i/t_a=1,05 ; h/Y=0,7 .

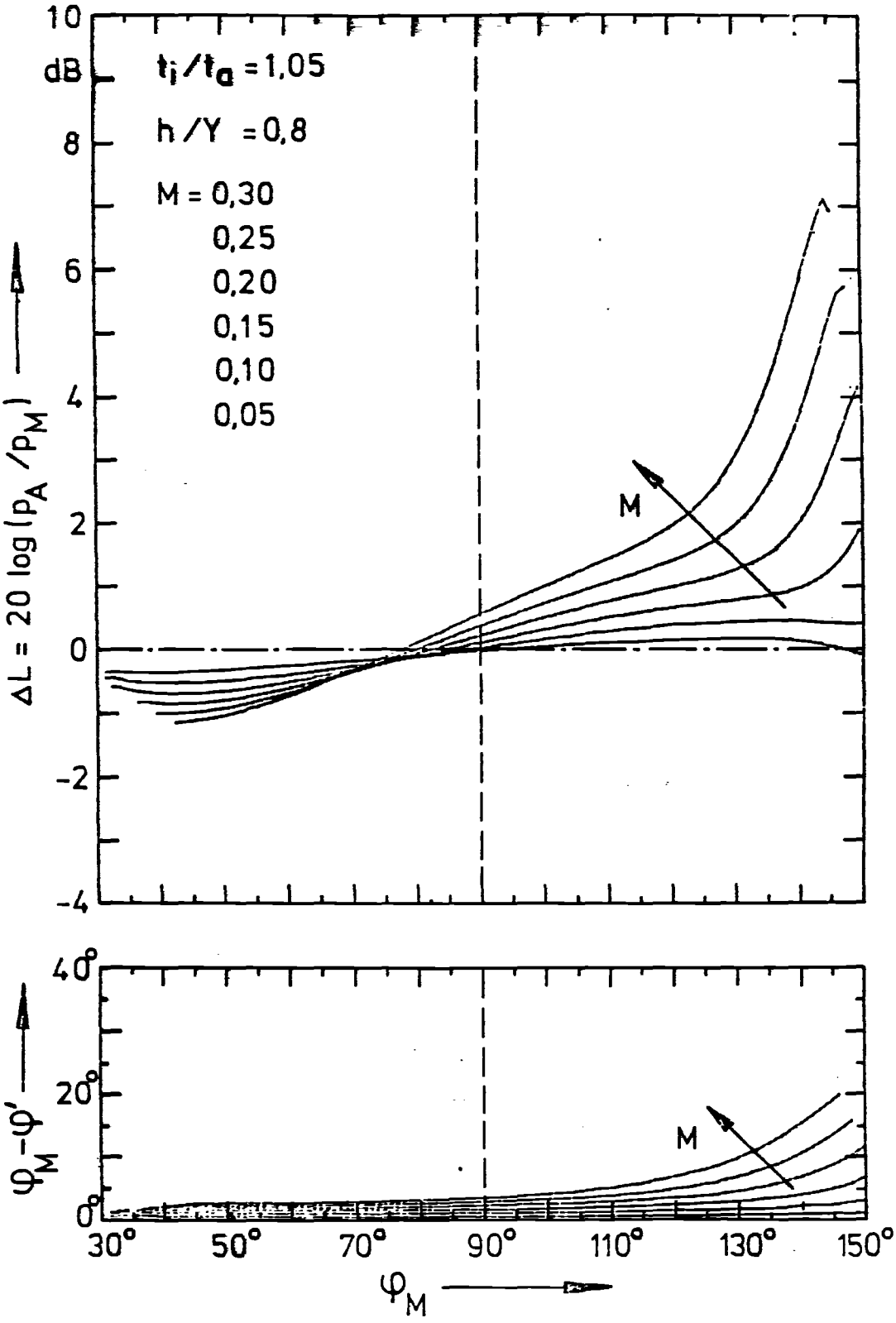

Figure 25. Amplitude and angle correction for different flow mach numbers for t_i/t_a=1,05 ; h/Y=0,8 .

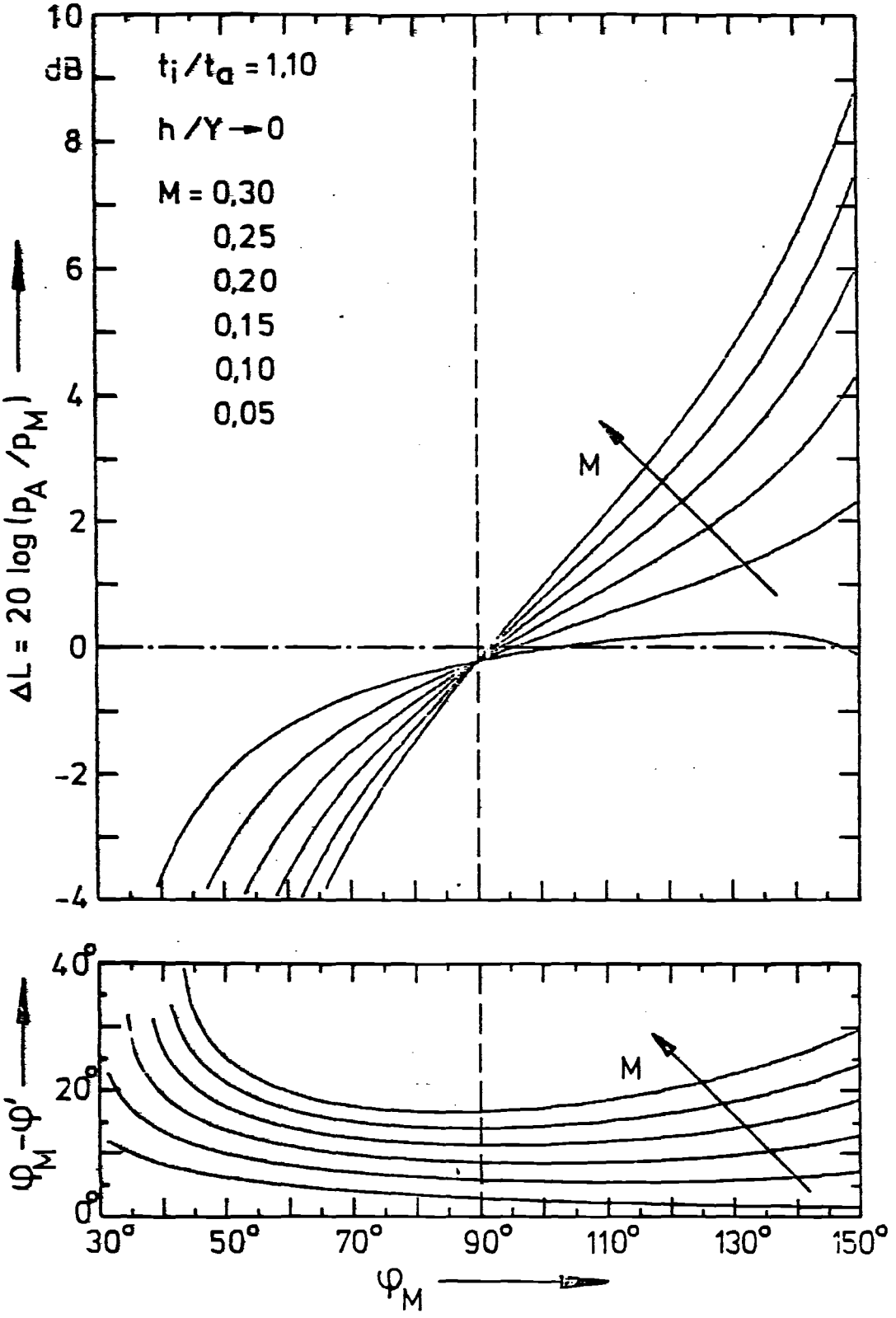

Figure 26. Amplitude and angle correction for different flow mach numbers for $t_i/t_a = 1{,}10$; $h/Y \to 0$.

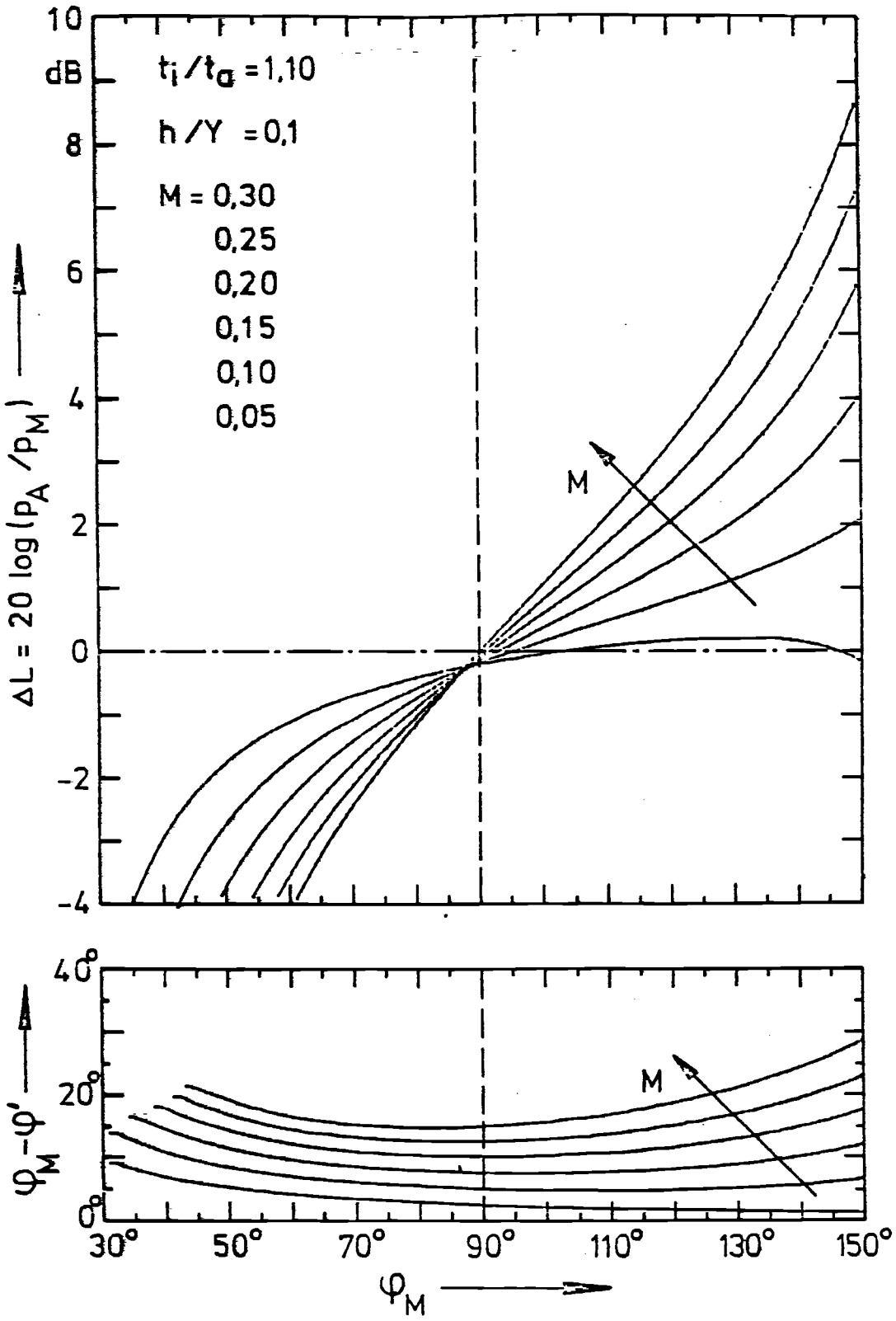

e 27. [illegible] correction for different flow mach [illegible] t_i/t_a=1,10 ; h/Y=0,1 .

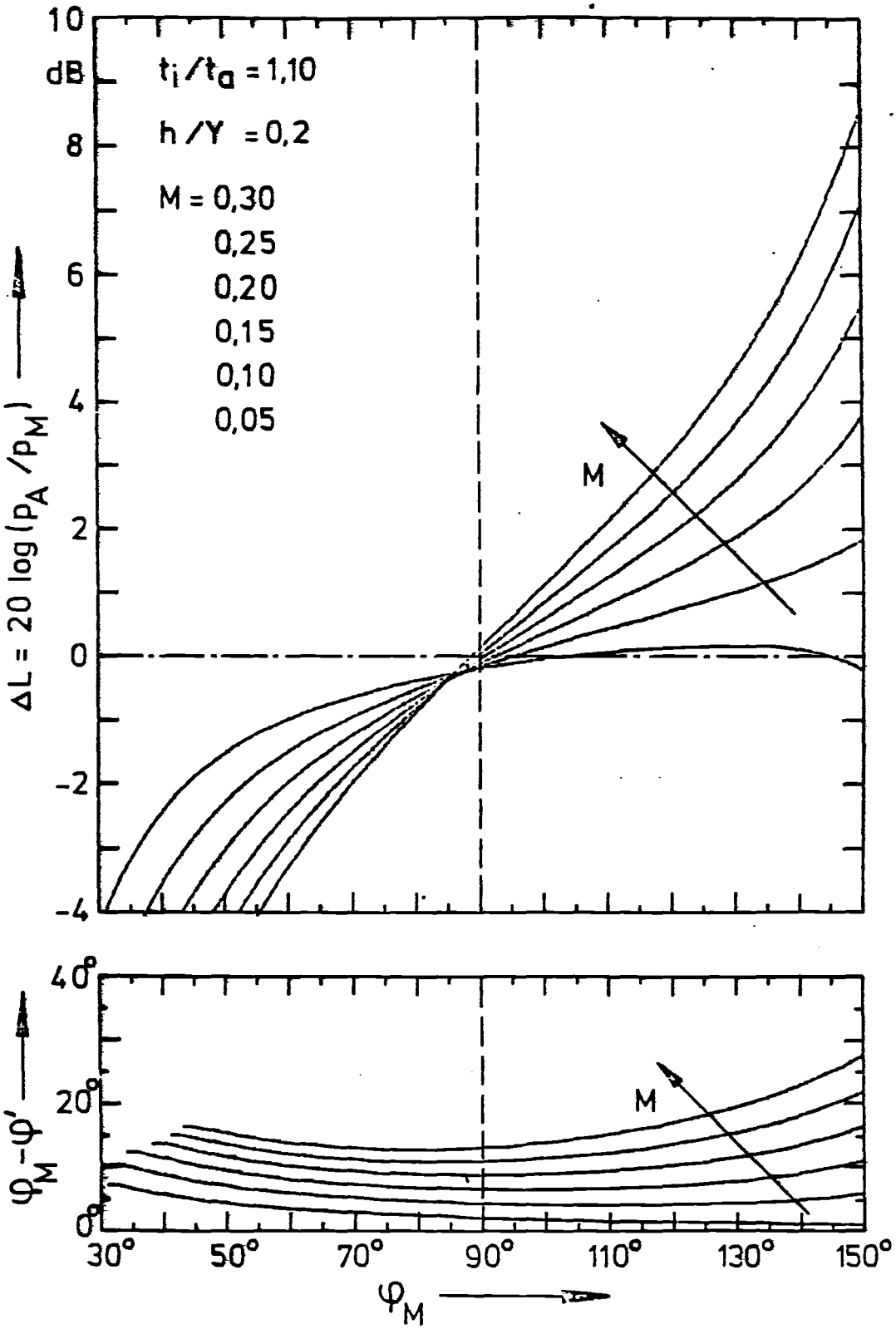

28. [illegible] angle correction for different flow mach
[illegible] for t_i/t_a=1,10 ; h/Y=0,2 .

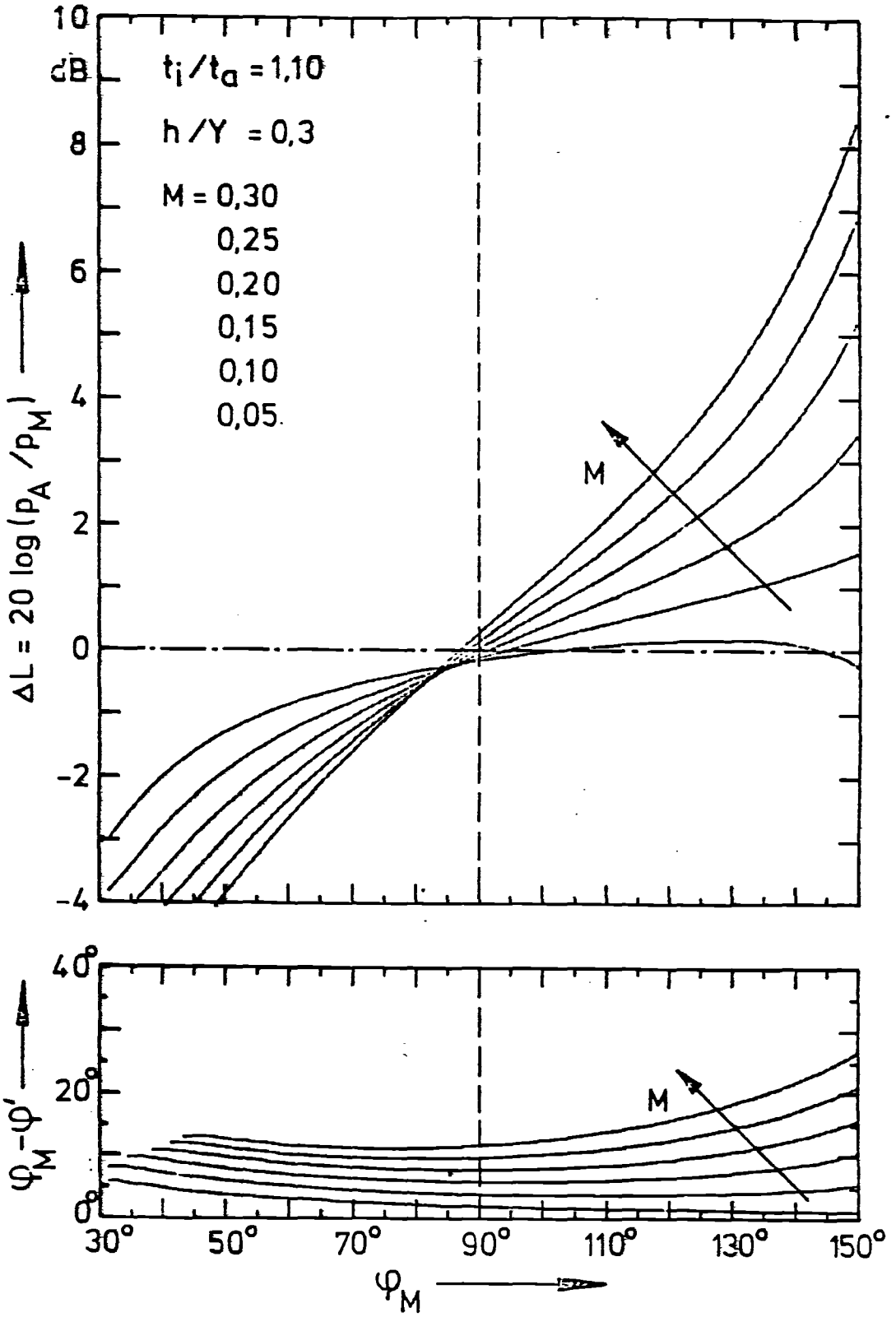

Figure 29. Amplitude and angle correction for different flow mach numbers for t_i/t_a=1,10 ; h/Y=0,3.

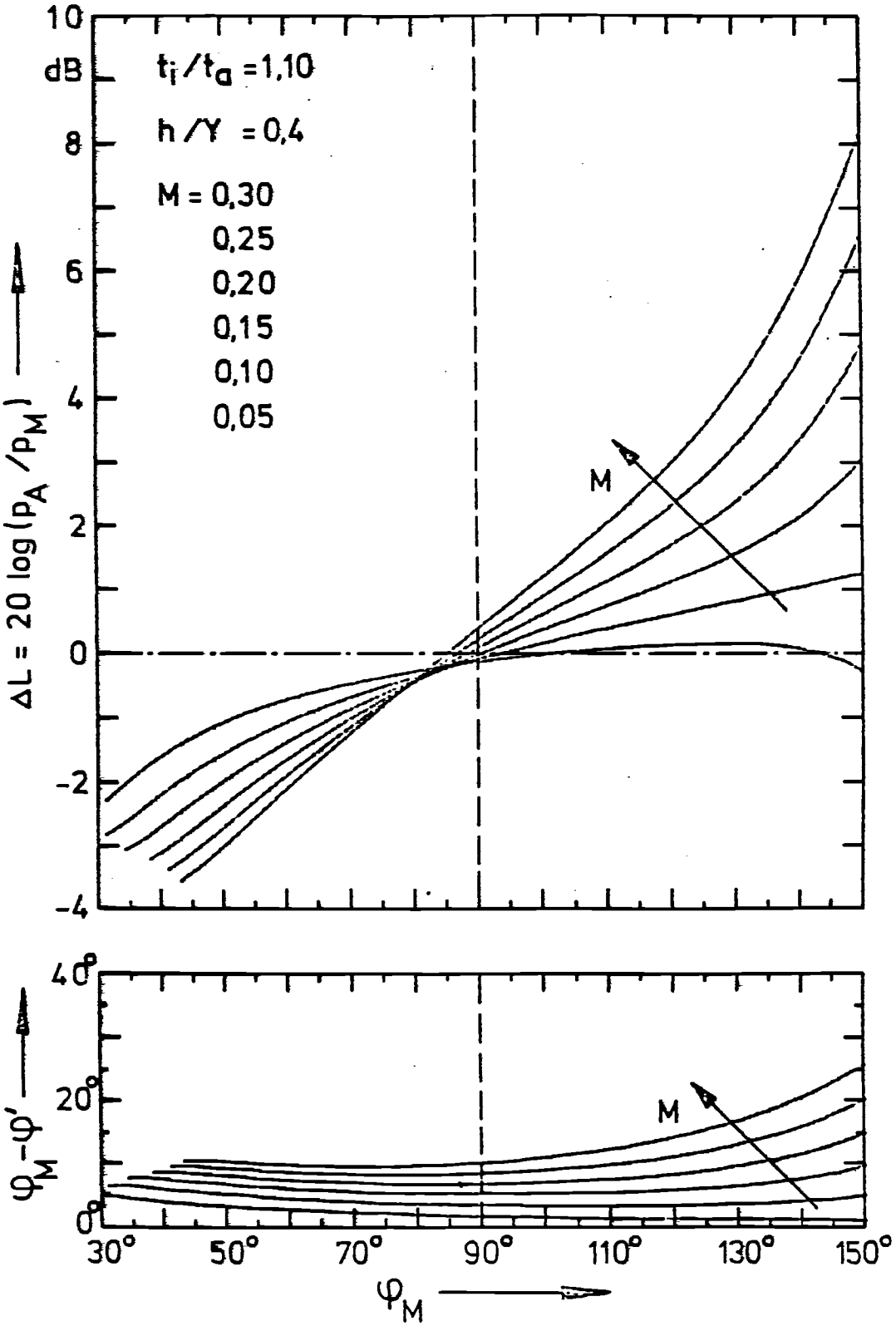

Figure 30. Amplitude and angle correction for different flow mach numbers for t_i/t_a=1,10 ; h/Y=0,4 .

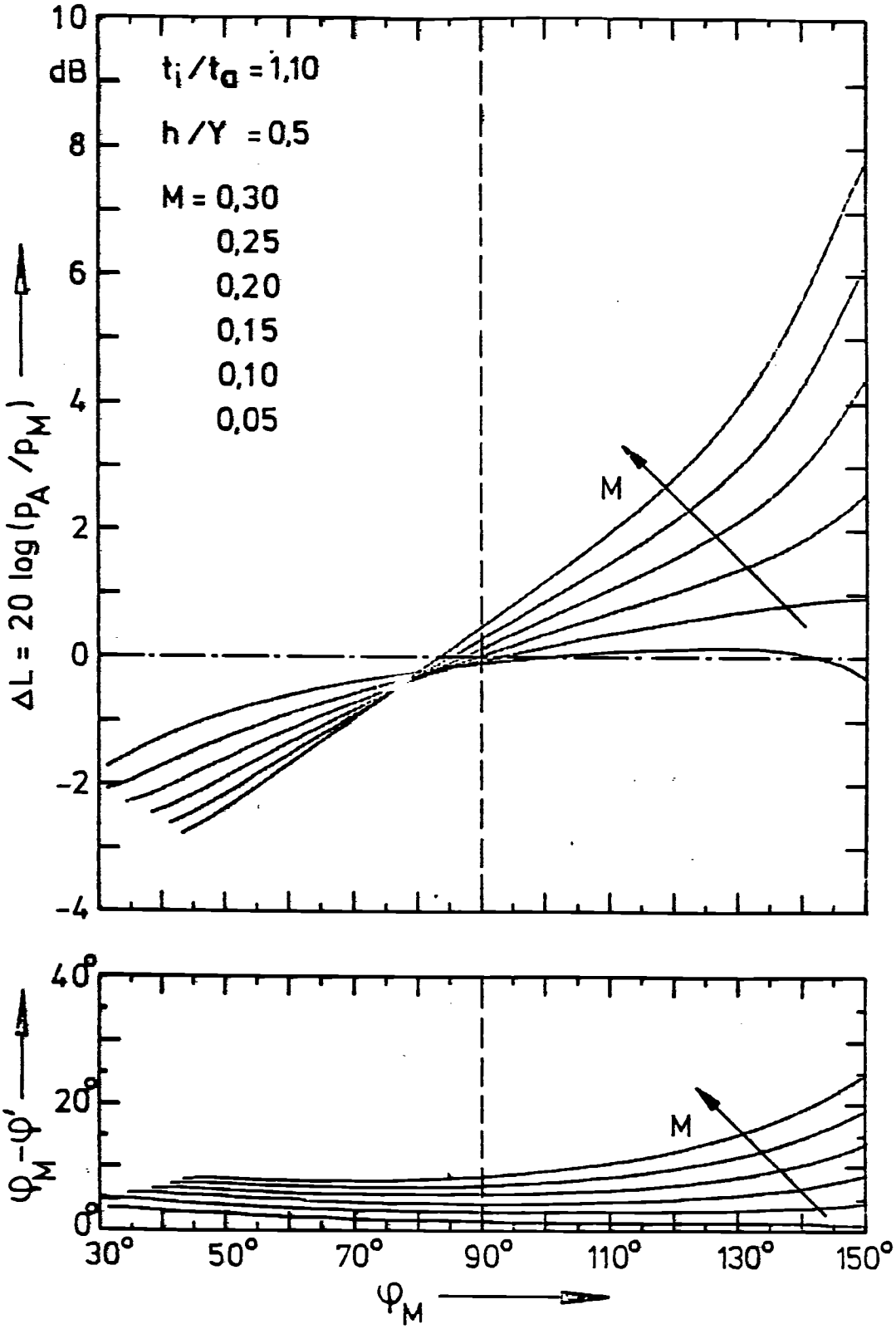

Figure 31 Amplitude and angle correction for different flow mach numbers for t_i/t_a=1,10 ; h/Y=0,5 .

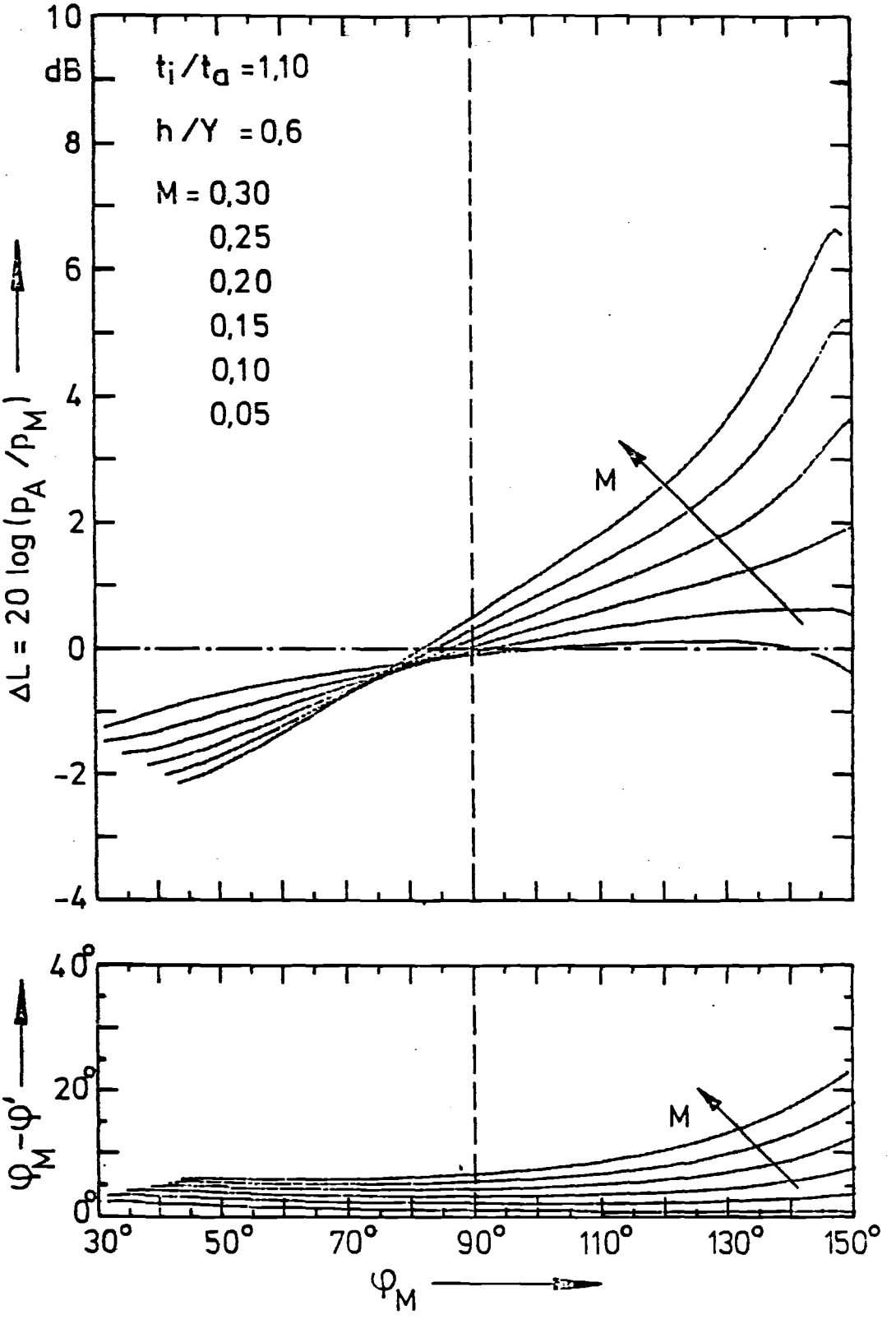

Figure 32 [illegible] w each

t_i/t_a=1,10 ; h/Y=0,6 .

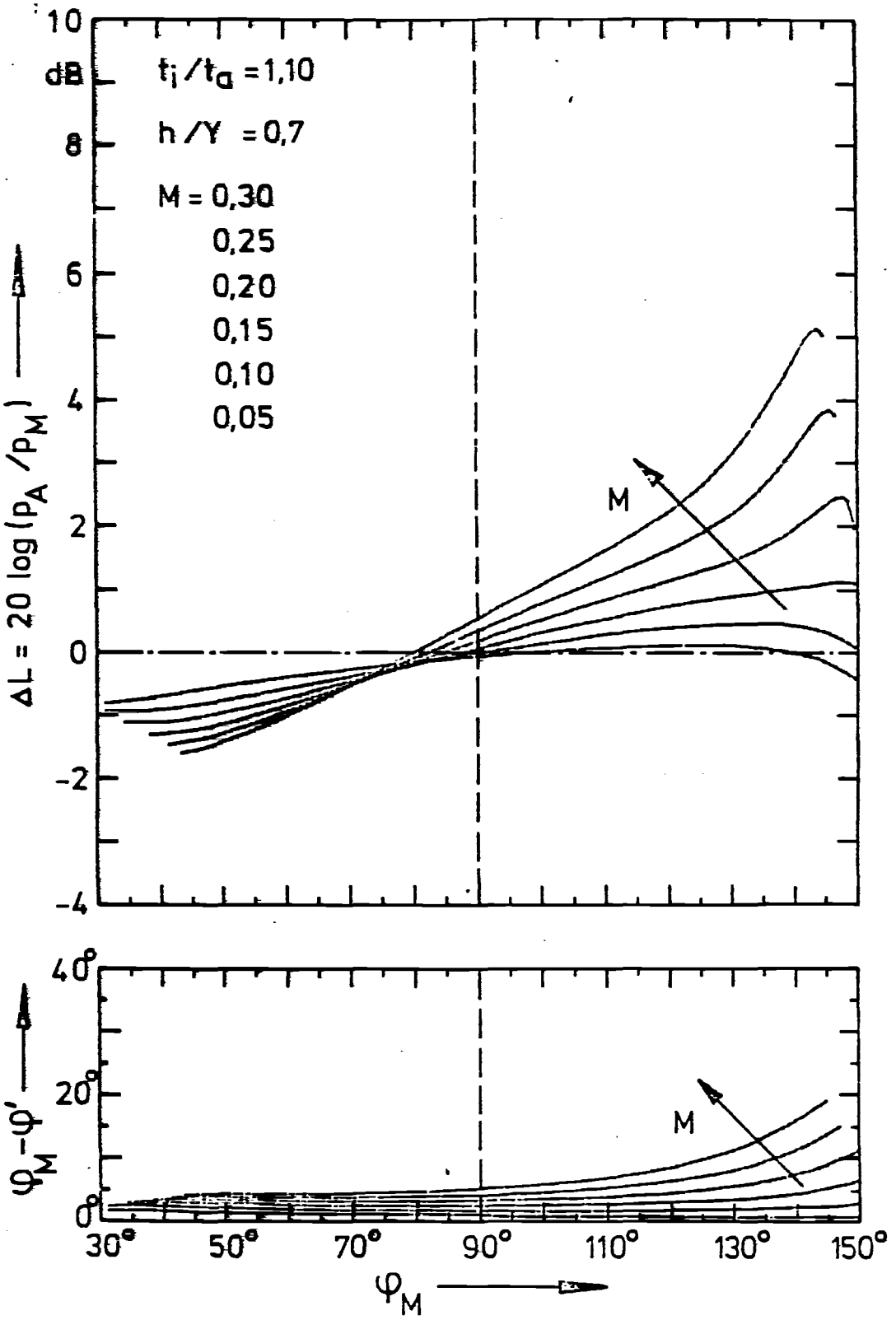

Figure 33. Sound pressure level correction for different flow mach numbers for t_i/t_a=1,10 ; h/Y=0,7 .

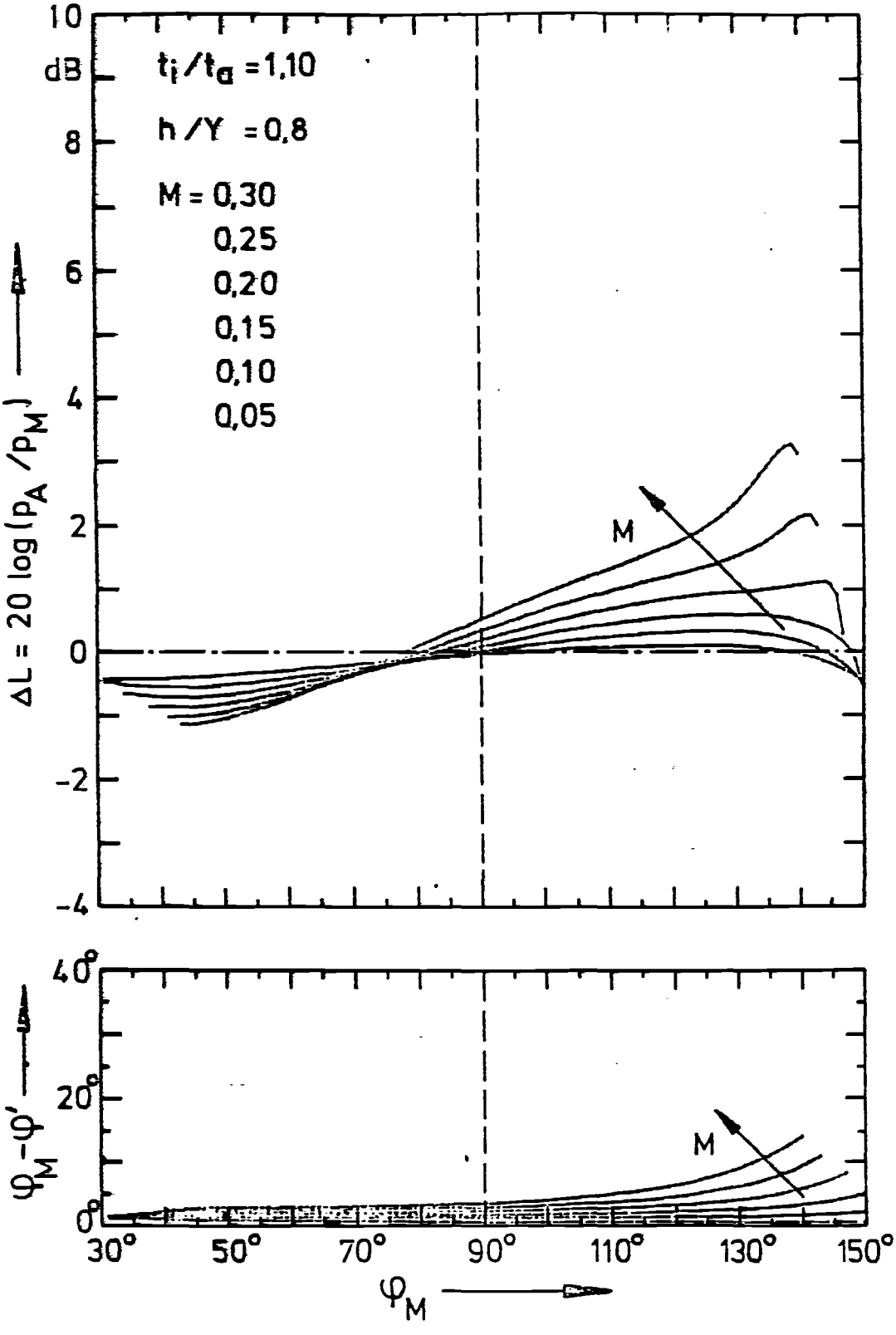

Figure 34. Amplitude and angle variation for different flow mach numbers for t_i/t_a=1,10 ; h/Y=0,8 .

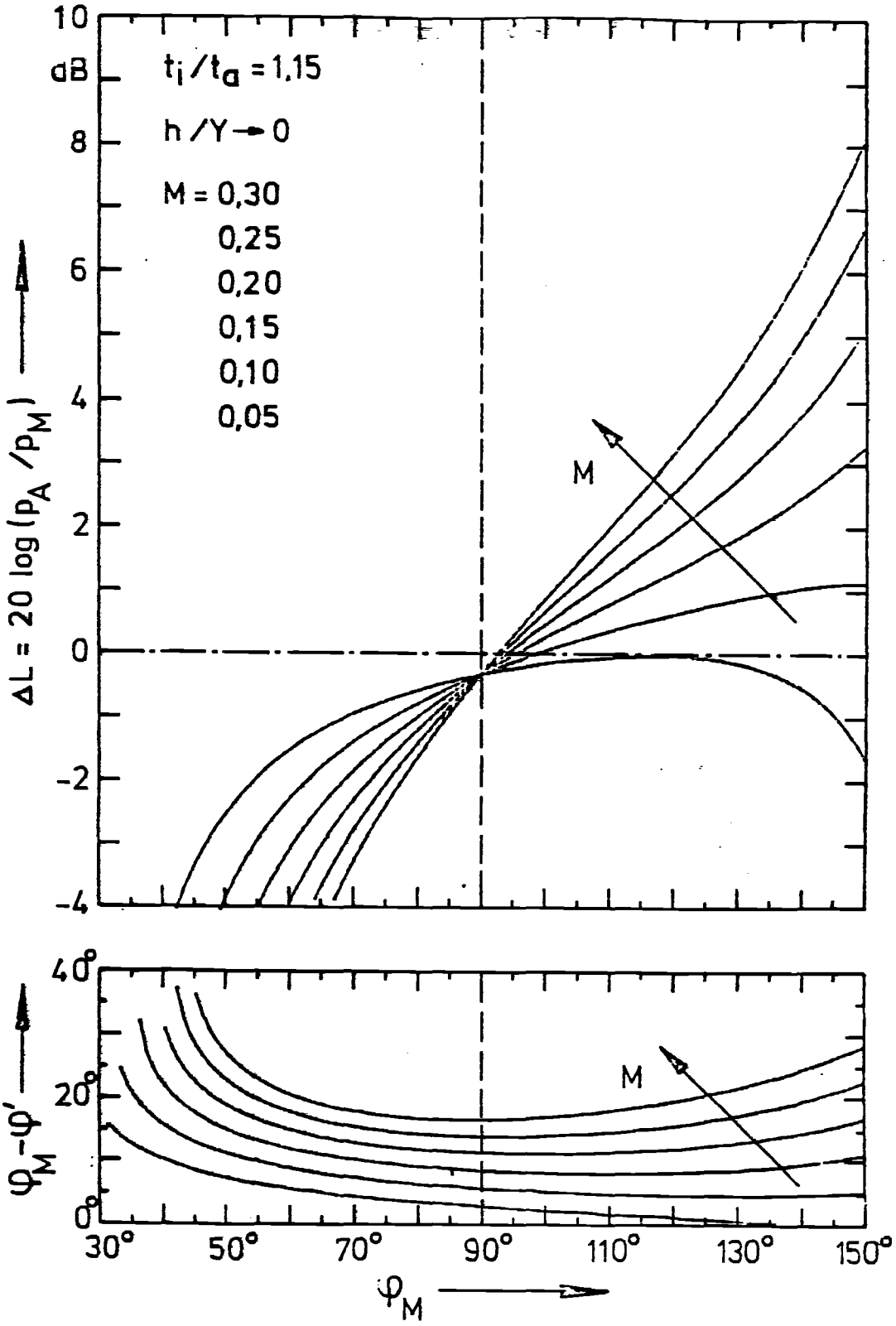

Figure 35. Amplitude and angle [illegible] for $t_i/t_a = 1{,}15$; $h/Y \to 0$

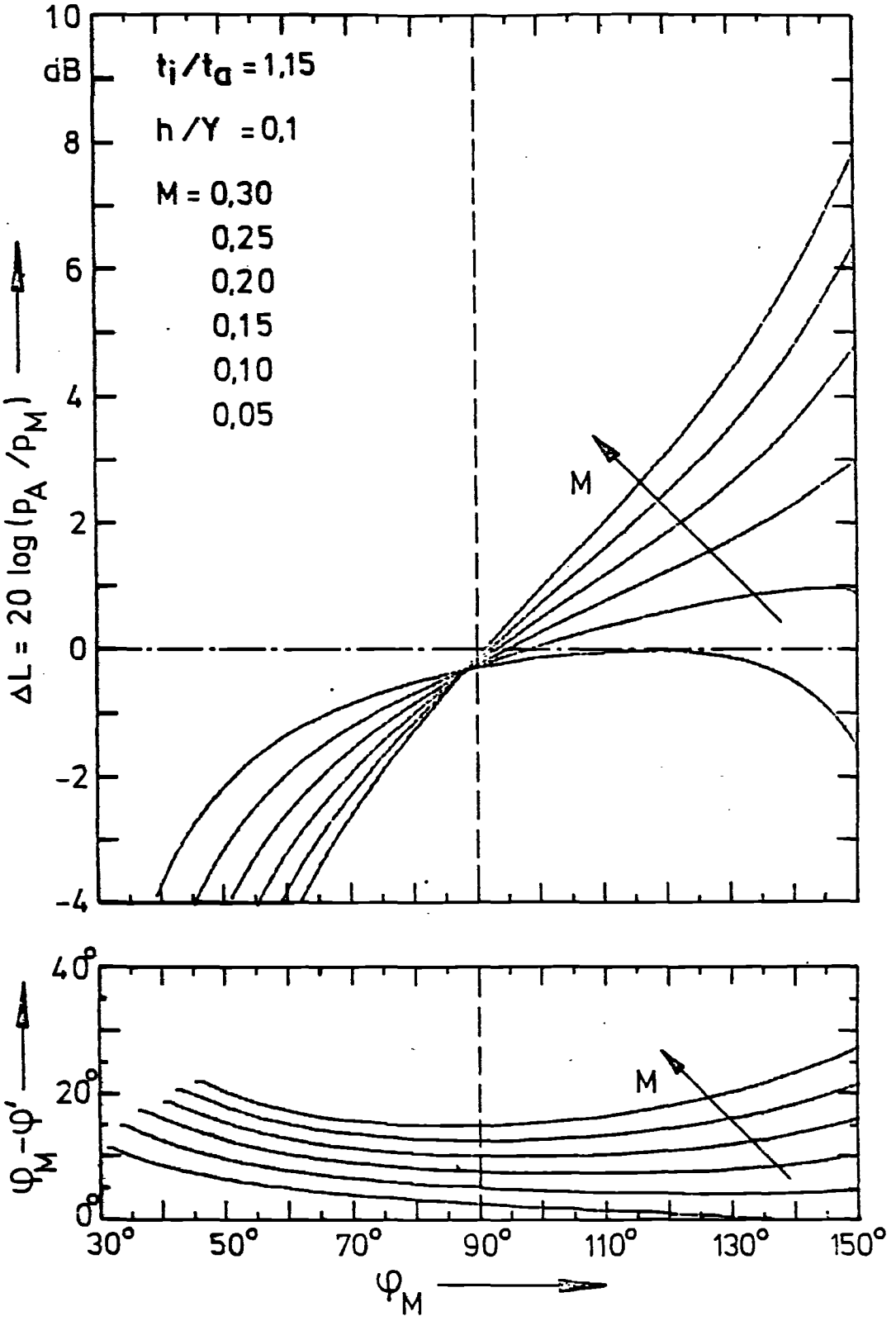

Figure 36. Amplitude and angle [illegible] Mach [illegible] with numbers for t_i/t_a=1,15 ; h/Y=0,1

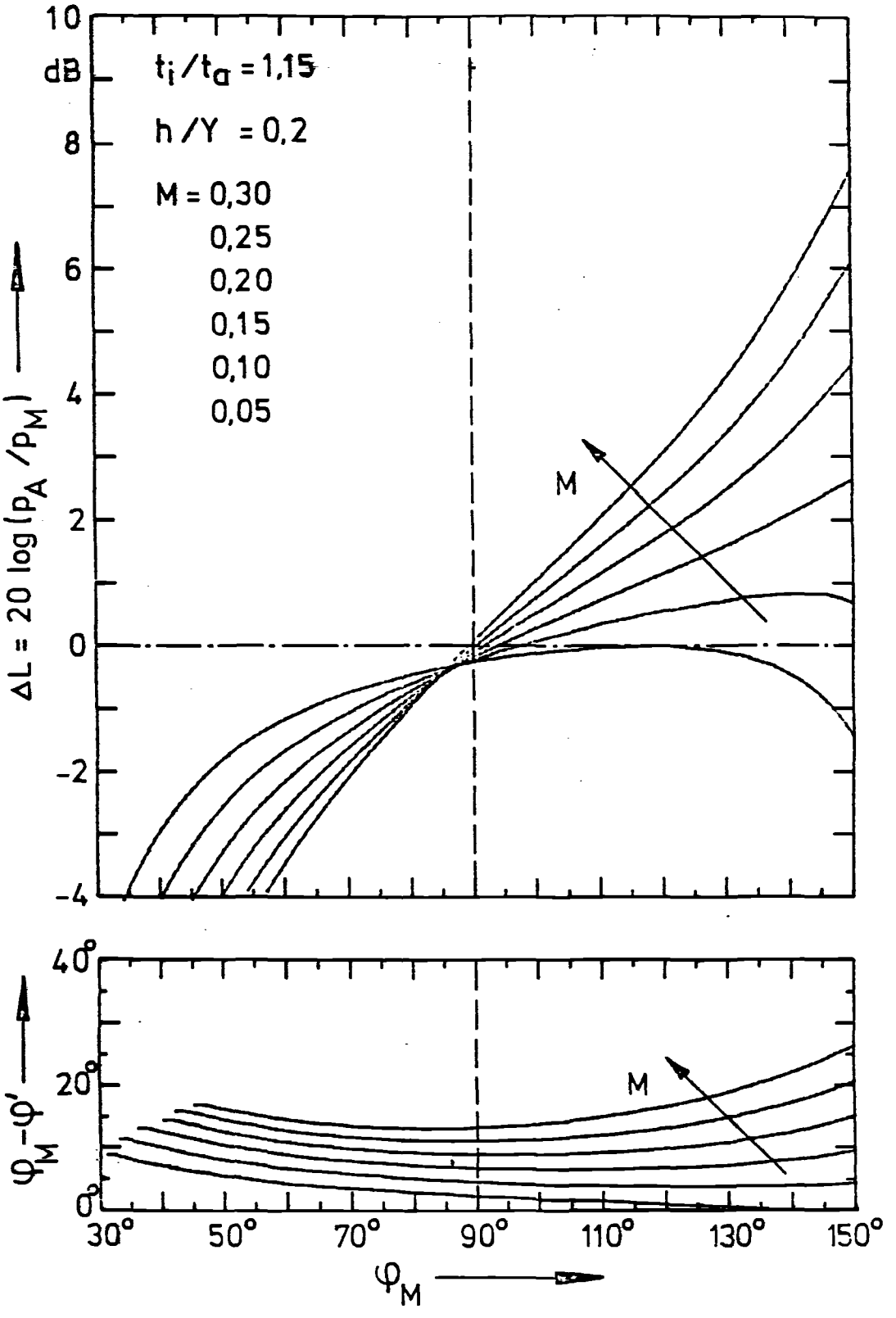

Figure 37. Amplitude and angle correction for different flow mach numbers for t_i/t_a=1,15 ; h/Y=0,2 .

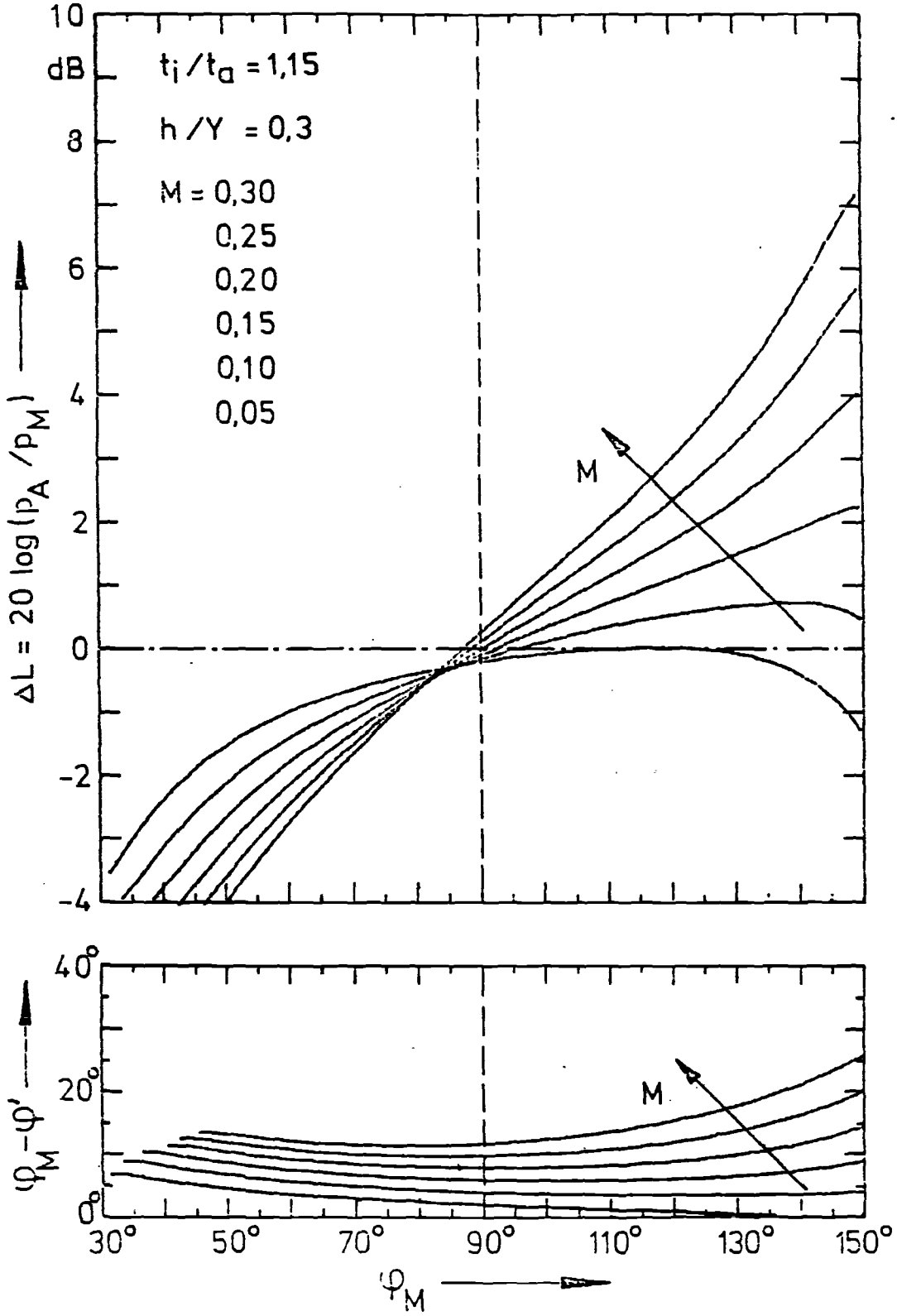

Figure 38. Amplitude and angle correction for different flow Mach numbers for t_i/t_a=1,15 ; h/Y=0,3 .

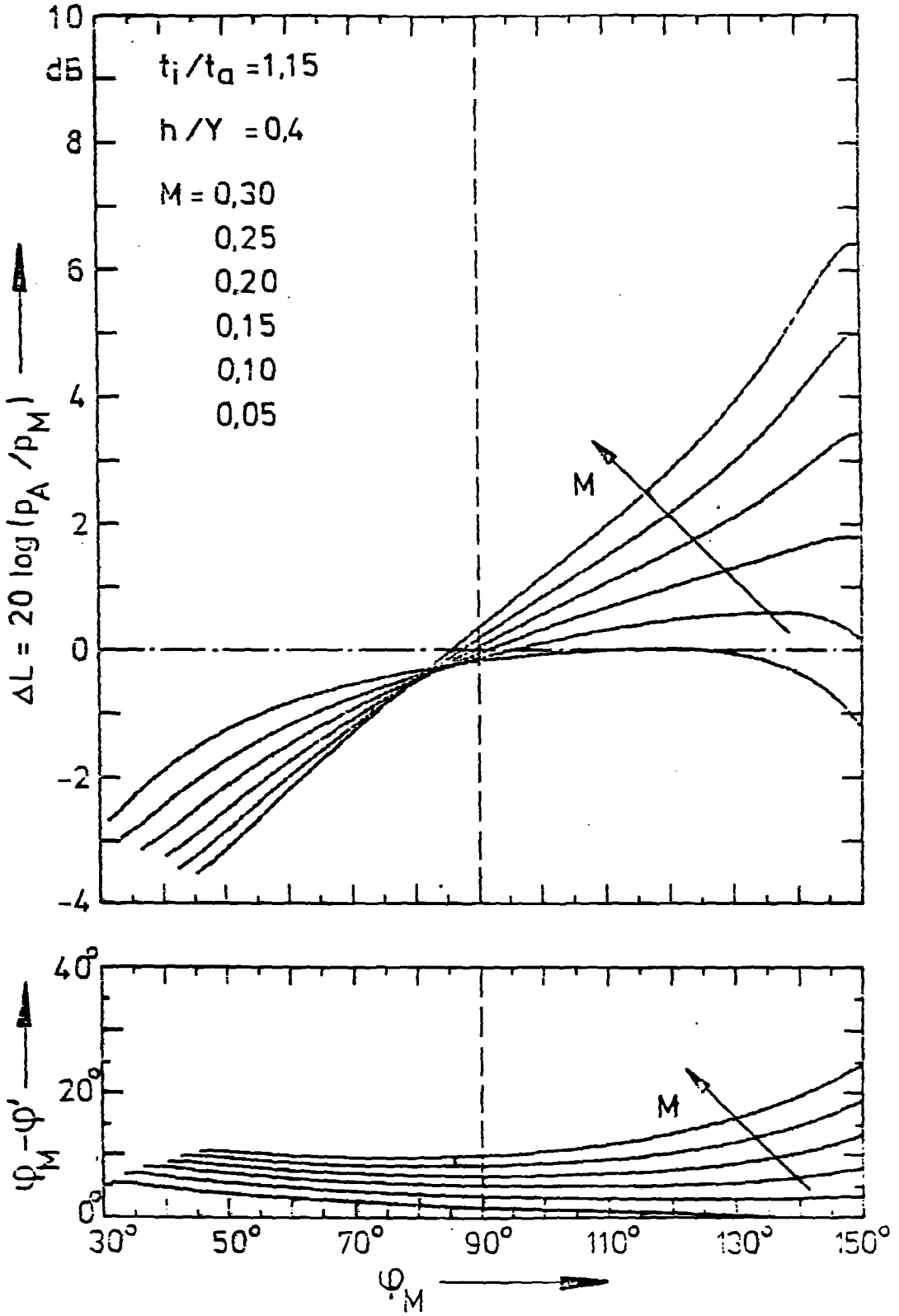

Fig. 39. [illegible] t_i/t_a=1,15 ; h/Y=0,4 .

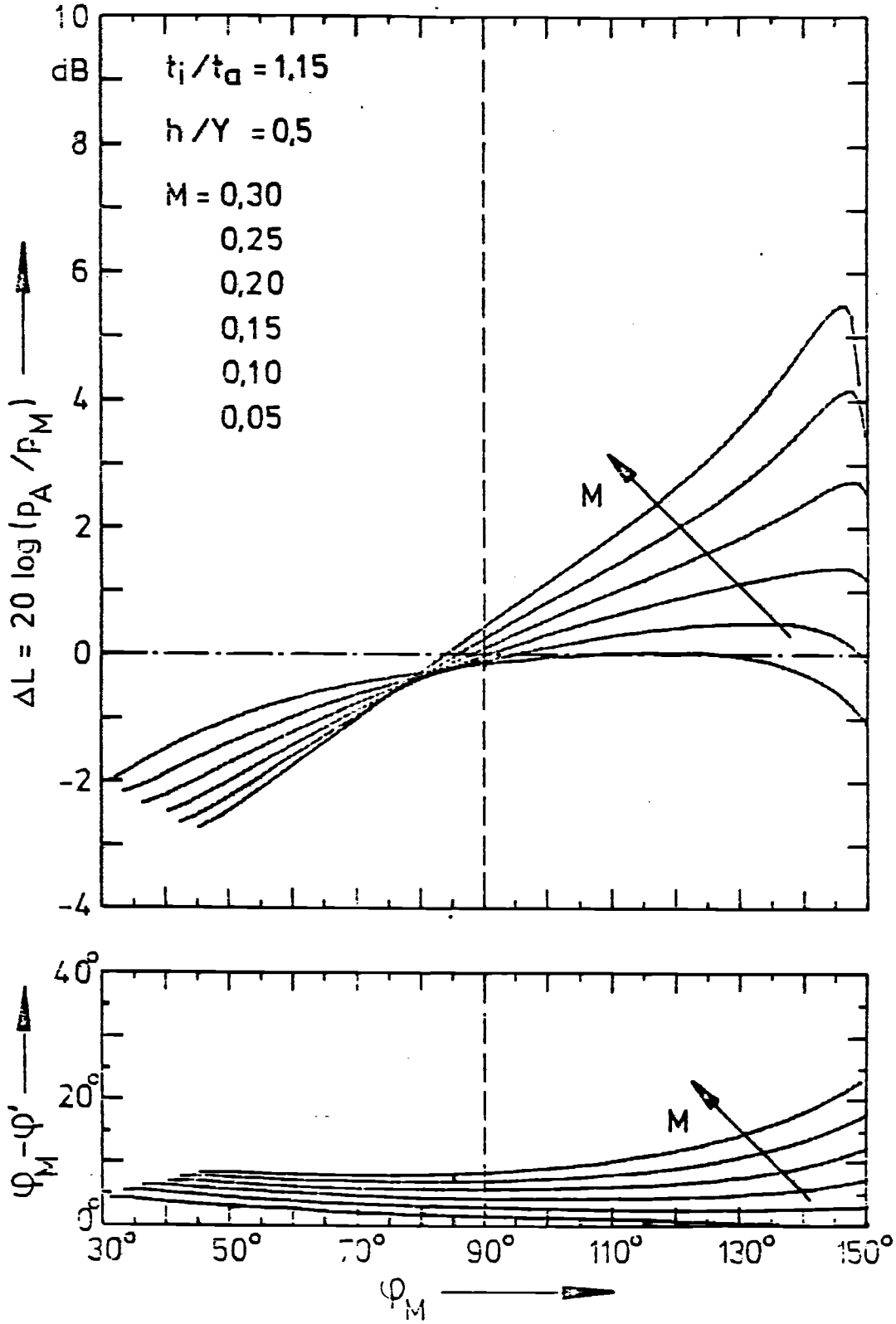

Figure 40 Amplitude and angle correction for different flow mach numbers for t_i/t_a=1,15 ; h/Y=0,5 .

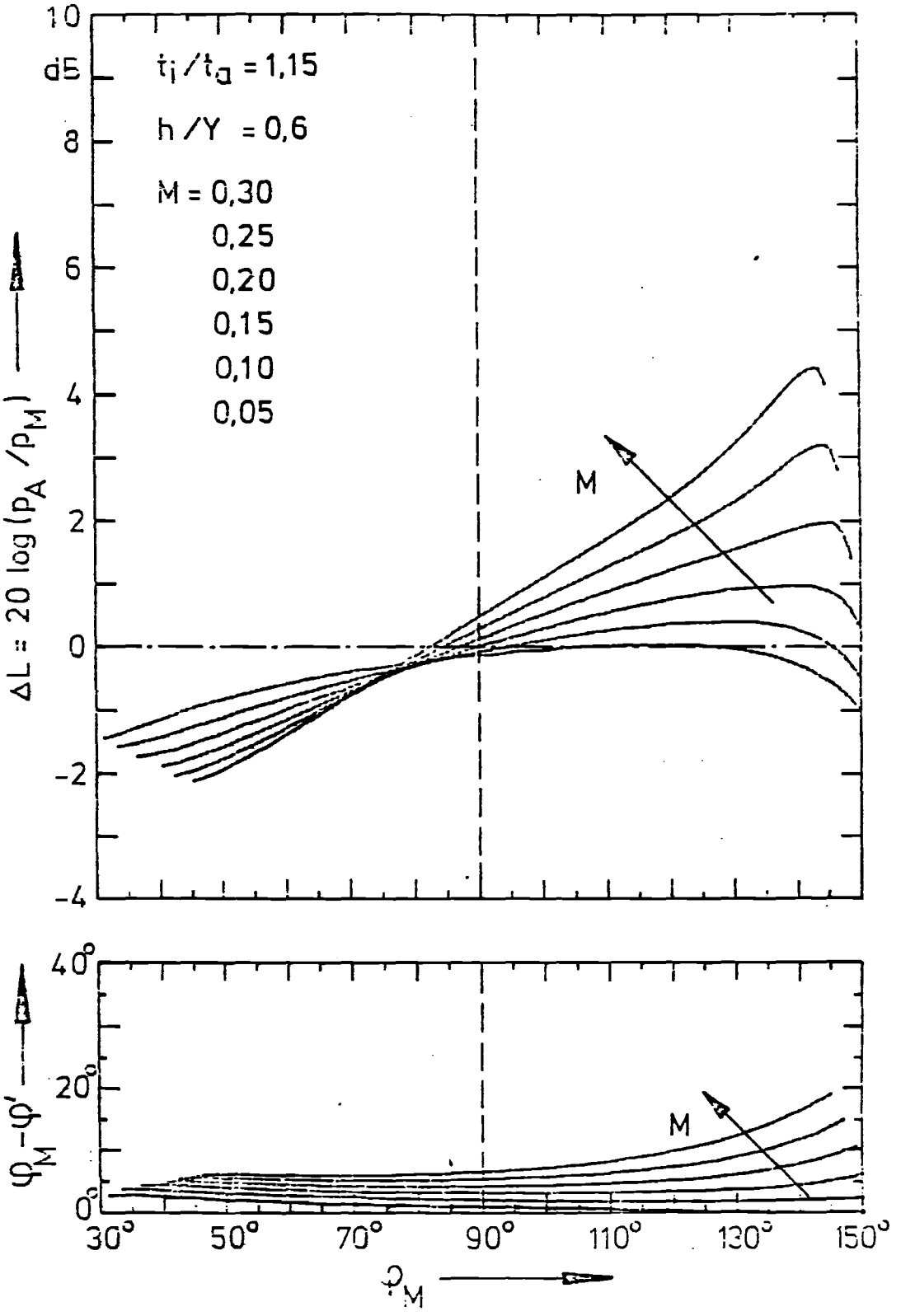

Fig. 41 Amplitude and angle correction for different flow mach numbers for t_i/t_a=1,15 ; h/Y=0,6 .

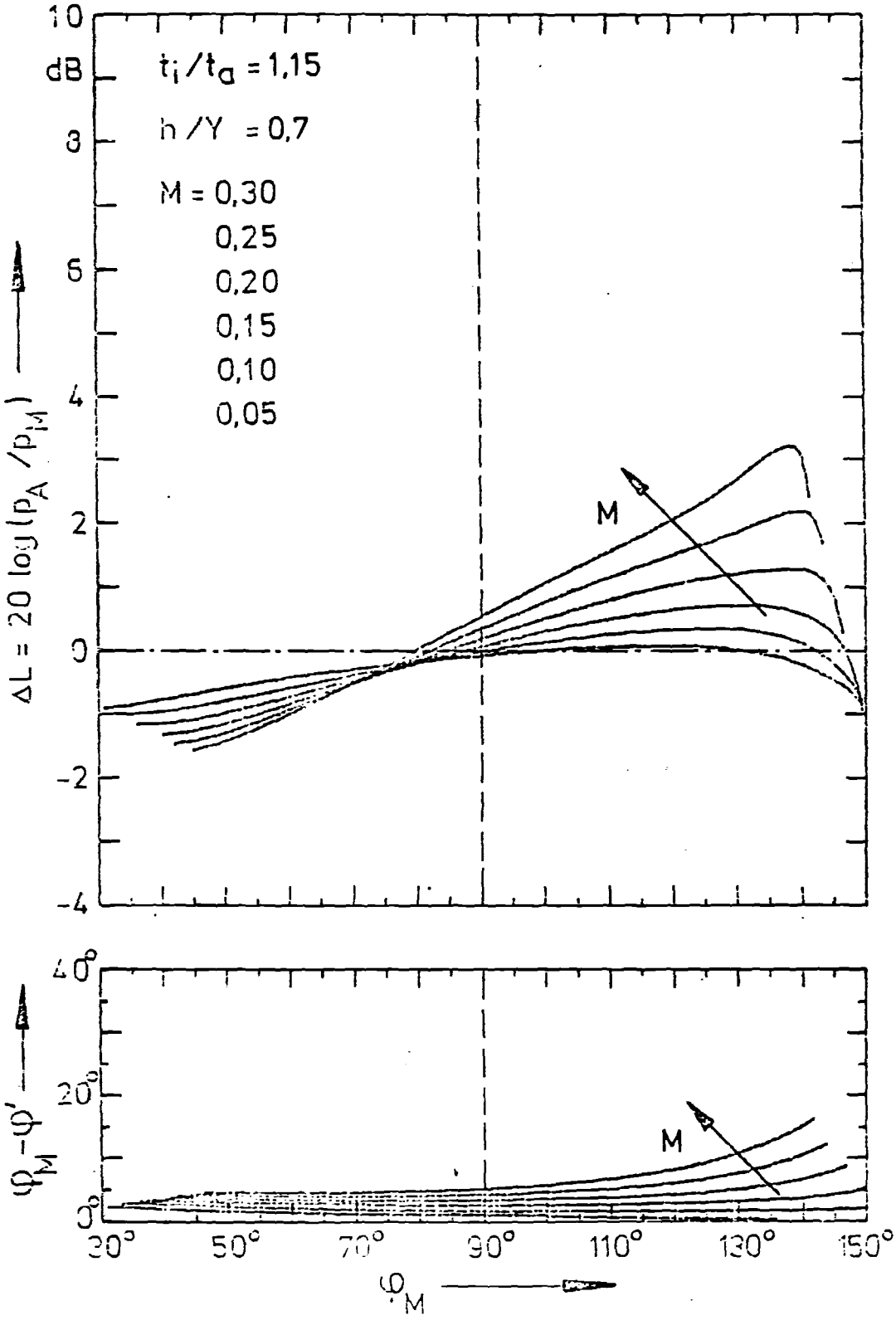

42

t_i/t_a=1,15 ; h/Y=0,7

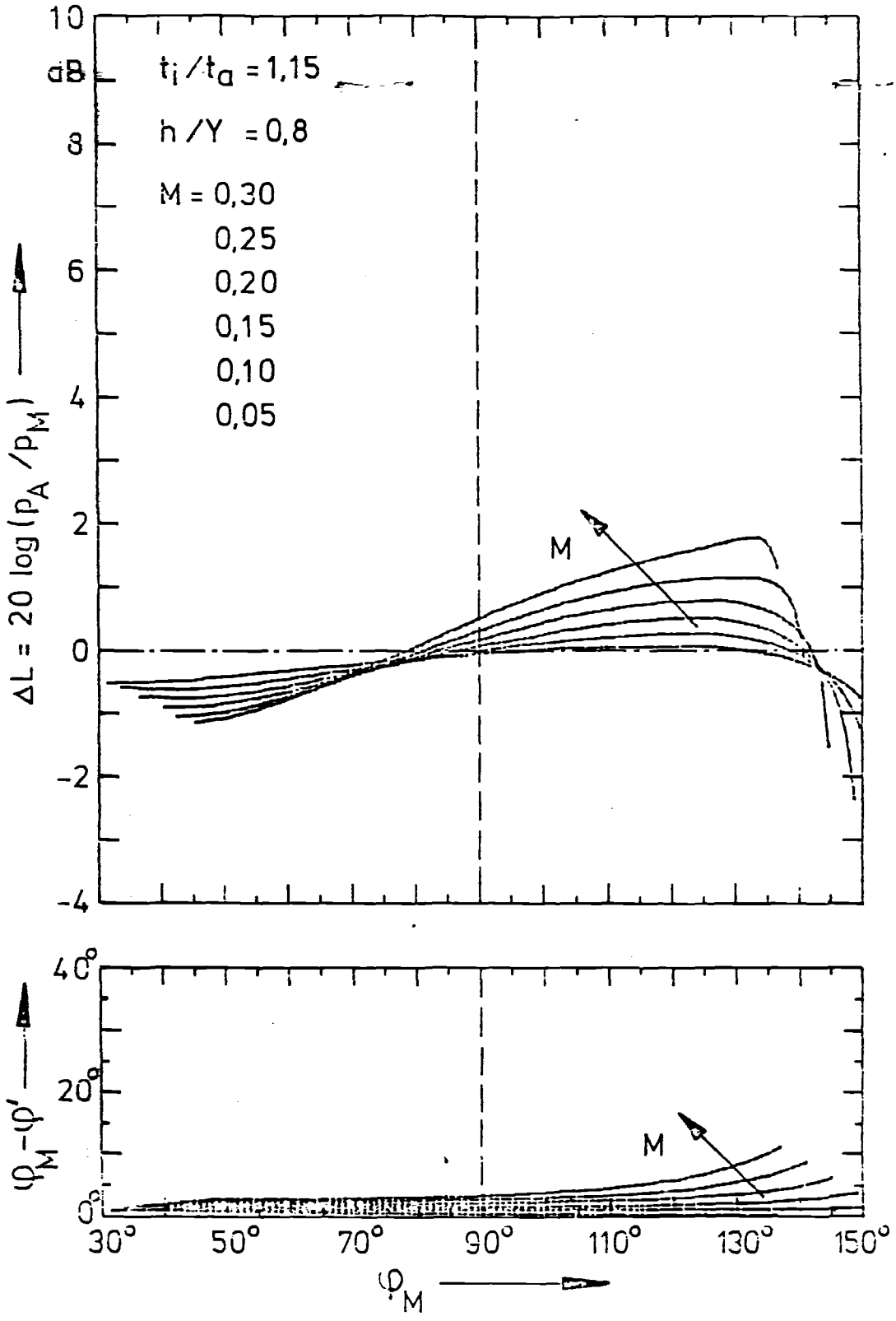

Figure 43. Amplitude and angle correction for different Mach numbers for $t_i/t_a = 1,15$; $h/Y = 0,8$.